Synergistic effects of temperature and light affect the relationship between Taonia atomaria and its epibacterial community: a controlled conditions study

Benoit Paix, Philippe Potin, Gaëtan Schires, Christophe Le Poupon, B. Misson, Catherine Leblanc, Gérald Culioli, Jean-françois Briand

Synergistic effects of temperature and light affect the relationship between *Taonia atomaria* and its epibacterial community: a controlled conditions study

Benoit Paix[a,1], Philippe Potin[b], Gaëtan Schires[c], Christophe Le Poupon[d], Benjamin Misson[d], Catherine Leblanc[b], Gérald Culioli[a,2,*] and Jean-François Briand[a,*]

[a]*Université de Toulon, Laboratoire MAPIEM, EA 4323, La Garde, France*

[b]*Sorbonne Université, CNRS, Integrative Biology of Marine Models (LBI2M), UMR 8227, Station Biologique de Roscoff (SBR), Roscoff, France*

[c]*Sorbonne Université, CNRS, Center for Biological Marine Ressources (CRBM), FR 2424, Station Biologique de Roscoff (SBR), Roscoff, France*

[d]*Université de Toulon, Aix Marseille Université, CNRS, IRD, Mediterranean Institute of Oceanography (MIO), UM110, La Garde, France*

*corresponding authors: briand@univ-tln.fr, gerald.culioli@univ-avignon.fr

Running head: Temperature and light affect holobiont dynamics

[1] New affiliation: *Marine Biodiversity, Naturalis Biodiversity Center, Leiden, The Netherlands.*

[2] New affiliation: *Institut Méditerranéen de Biodiversité et d'Ecologie marine et continentale (IMBE), UMR CNRS-IRD-Avignon Université-Aix-Marseille Université, Avignon, France.*

Originality-Significance Statement

We developed an experimental set up using controlled conditions, supplied by natural seawater, to test an algal holobiont response to changes of temperature combined with those of irradiance over 14 days, and using a multi-omics approach coupling algal surface metabolomics and metabarcoding.

Summary

In a context of global warming, this study aimed to assess the effect of temperature and irradiance on the macroalgal *Taonia atomaria* holobiont dynamics. We developed an experimental set up using aquaria supplied by natural seawater with three temperatures combined with three irradiances. The holobiont response was monitored over 14 days using a multi-omics approach coupling algal surface metabolomics and metabarcoding. Both temperature and irradiance appeared to shape the microbiota and the surface metabolome, but with a distinct temporality. Epibacterial community firstly changed according to temperature, and later in relation to irradiance, while the opposite occurred for the surface metabolome. An increased temperature revealed a decreasing richness of the epiphytic community together with an increase of several bacterial taxa. Irradiance changes appeared to quickly impact surface metabolites production linked with the algal host photosynthesis (e.g. mannitol, fucoxanthin, DMSP), which was hypothesized to explain modifications of the structure of the epiphytic community. Algal host may also directly adapt its surface metabolome to changing temperature with time (e.g. lipids content) but also in response to changing microbiota (e.g. chemical defenses). Finally, this study brought new insights highlighting complex direct and indirect responses of seaweeds and their associated microbiota under changing environments.

Keywords: holobiont, surface metabolome, surface microbiota, metabolomics, controlled condition experiments, multi-omics

Introduction

As marine holobionts, macroalgae are known to establish intimate relationships with their epiphytic microbiota (Hollants et al., 2013). Notably, macroalgae are capable of controlling their epibacterial consortia through chemical defenses as well as chemoattractants released at their surface (Harder et al., 2012; Wahl et al., 2012; Wichard et al., 2015). Such negative or positive chemical mediations play an important role for the host physiology and, for example, can be associated to immune or development processes (Wichard and Beemelmanns, 2018). As sessile organisms in intertidal and infralittoral zones, marine macroalgae are subject to many environmental changes often linked to anthropogenic stresses, such as global warming or marine coastal pollution (Dittami et al., 2014; van der Loos et al., 2019). Concerns are notably raised to understand how climate changes will drive seaweed-bacteria interactions in the future (Campbell et al., 2011; Egan et al., 2014; Egan and Gardiner, 2016). As for other marine holobionts such as corals and sponges, temperature increase and seawater acidification are the most investigated factors for macroalgae in this context of global changes (van der Loos et al., 2019).

Among macroalgae, the bleaching disease of the Rhodophyta *Delisea pulchra* has been directly correlated to the temperature increase. This alga produces chemical defenses, identified as halogenated furanones, known to act as quorum sensing inhibitors and protecting the seaweed against bleaching disease (Maximilien et al., 1998; Harder et al., 2012). However, algae that bleach in response to water temperature increases, features lower levels of these defenses (Campbell et al., 2011; Case et al., 2011). In these specific conditions, several opportunistic bacteria (e.g. *Nautella italica* and *Phaeobacter* sp.) are observed at the algal surface and have been proposed to be involved in the bleaching phenomenon (Case et al., 2011; Fernandes et al., 2011; Campbell et al., 2014; Kumar et al., 2016). Even if temperature alone failed to explain the bleaching disease (Zozaya-Valdés et al., 2016), a global decrease of macroalgal health and dysbiosis should be a plausible scenario to anticipate in the context of global warming (Egan et al., 2014).

In the last few years, the combined effect of the rise of temperature and seawater acidification on macroalgal physiology and surface microbiota has been increasingly studied through controlled conditions experiments. While for the Chlorophyta *Caulerpa taxifolia* mitigating effects

are observed (Roth-Schulze et al., 2018), predicted future climate conditions influence the microbiota structure for the Phaeophyceae *Eklonia radiata* (Qiu et al., 2019), *Macrocystis pyrifera* (Minich et al., 2018), *Fucus vesiculosus forma mytili* (Mensch et al., 2016) and the Rhodophyta *Amphiroa gracilis* (Huggett et al., 2018). Moreover, the host physiology is also disturbed with blistered tissues and reduced photosynthetic efficiency for *E. radiata*, bleaching disease for *A. gracilis* and growth reduction for *C. taxifolia*, *M. pyrifera*, and *F.v. mytili*. In the case of the well-studied brown alga *Fucus vesiculosus* (Saha et al., 2014), effects of light and temperature have been investigated independently through the study of the surface concentrations of three metabolites [i.e. proline, dimethylsulfoniopropionate (DMSP) and fucoxanthin] known as bacterial settlement inhibitors. The potential effect of the variations of these surface compounds on the epibacterial community structure has been also studied. To our knowledge, this is the only mesocosm study focusing simultaneously on surface microbiota and metabolites, with chemical analyses specifically limited on these three compounds. The direct impact of both parameters appears relatively limited on these metabolites, but variations of their surface concentrations could possibly modify the relative proportions of major bacterial families, as shown when DMSP concentration increases. However, if light and temperature seem to be key factors for shaping the overall epibacterial community of marine algae, their combined effects have not been investigated so far in controlled laboratory conditions, especially in relationships with the whole surface chemical environment.

While most surface metabolites playing a potential role in the surface microbiome assembly (such as DMSP or fucoxanthin) were presumably attributed to the host production (Lachnit et al., 2010; Saha et al., 2011; Grosser et al., 2012; Saha et al., 2014), little is known on the relative importance of bioactive compounds from the epibacterial community at the holobiont scale. These later, could participate actively to the shift of a community structure, through antagonistic interactions within the microbiome for example (antibiotic, quorum quenching activities, …) (Wietz et al., 2013). One of the most clear evidence of the role of microbial secondary metabolites on the host was the morphogenesis-promoting factors required for the growth and morphogenesis in the case of the sea lettuce *Ulva* spp. (Ghaderiardakani et al., 2017, 2019).*Taonia atomaria* (Woodward) J. Agardh is an annual photophilic marine Phaeophyceae widely reported along the

Mediterranean and the NE Atlantic coasts (Guiry and Guiry, 2020). This seaweed is known to produce at its surface several compounds displaying anti-adhesion activities (e.g. gleenol and geranylgeranylglycerol) (Othmani et al., 2016) against a panel of marine bacteria. Such metabolites have been hypothesized to be part of the algal chemical defenses and involved in the selection of a specific epibacterial community. Furthermore, strong seasonal correlations occur, notably during spring and summer, between specific surface metabolites and some epibacterial taxa (Paix et al., 2019). In the light of these results and those previously obtained for the algal model *F.v. mytili*, the increase of temperature has been hypothesized as a key factor shaping the dynamics of such interactions. However, in the case of *T. atomaria,* the field studies have not delineated the respective effects of colinear factors such as temperature and light. Due to their temporal covariations, their relative importance is now questioned according to the important seasonal effect observed as part of *in situ* studies (Paix et al., 2019, *submitted*).

The objective of this "controlled conditions experiment" was to decipher the respective and synergistic effects of temperature and irradiance on the interactions between *T. atomaria* and its epibacterial community. The temperature values were chosen according to the natural *in situ* variations observed during the summer, when the epibiotic community is stabilized (Paix et al., 2019). As temperatures follow an increase and then a decrease from the beginning to the end of the summer along coasts of north Brittany, three different temperatures were chosen: an ambient one corresponding to the field measures in June (18°C named AT for ambient temperature), together with a higher and a lower ones corresponding to the extremes observed within this period (13°C and 22°C named LT and HT, respectively for low and high temperatures). Additionally, the HT condition corresponded to +4°C compared to the AT condition, which suited with the predictions made for 2081-20100 with the RCP 8.5 model in the Global Change context (Collins et al., 2013). The different irradiance conditions were chosen in accordance with *in situ* variations mainly linked to the different depths, according to the changing tide conditions, and the range of photosynthetic saturation points (I_k) previously described in the literature for brown seaweeds. Located at the limit between the intertidal and the infralittoral zones, *Taonia* populations on Brittany coasts can vary from 2 to 8m depth. Consequently, contrasted degrees of light penetration (according to the tide changes in this environment) were considered (Roberts

et al., 2018). Additionally, the three light treatments (20, 120 and 350 μmol photons m^{-2} s^{-1}, named LI, AI and HI, respectively for low, ambient and high irradiances) were chosen since the corresponding irradiance values were respectively located below, within and above the I_k range generally observed for brown seaweeds (100 - 200 μmol photons m^{-2} s^{-1}) (Forster and Dring, 1994; Hanelt et al., 1995; Murakami et al., 2004). Such a choice was considered in order to compare three different states of the seaweed based on its photosynthetic capacity.

These three temperatures and irradiances were combined and sampling was performed after three different times of incubation after the acclimatation period (t_1, t_2 and t_3: one day, one week and two weeks, respectively). The resulting surface microbiota and metabolome were subjected to a multi-omics analysis. Untargeted LC-(+)-ESI-MS metabolomics dedicated to the analysis of surface metabolites was coupled to 16S rRNA gene metabarcoding and flow cytometry, for the analysis of epiphytic prokaryotic dynamics.

Results

Physicochemical parameters

Several physicochemical parameters measured in the aquaria showed a low variability during the whole study, such as salinity, pH, dissolved O_2 levels, and $[Si(OH)_4]$ with mean values of 35.8 ppt [Standard deviation (SD) = ± 0.2 ppt], 8.1 (SD = ± 0.05), 90% (SD = ± 1.4%), and 1.93 μM (SD = ± 0.28 μM), respectively (Table S1). However, some parameters showed a higher variability, such as $[NO_3^-]$ and $[PO_4^{3-}]$ with mean values of 1.27 μM (SD = ±0.58 μM) and 0.209 μM (SD = ±0.097 μM), respectively. Significant changes appeared only for $[PO_4^{3-}]$ according to the three-way ANOVA test with the time factor only (Table S2), revealing an increase from t_1 to t_3 confirmed with a Tukey's test. No significant interaction between time, irradiance and temperature factors was observed according to three-way ANOVA tests (Table S2). Moreover, when comparing natural and aquaria seawater, only $[Si(OH)_4]$ exhibited significant differences (one-way ANOVA: $p < 0.05$), with mean values decreasing by a 3-fold factor from field to controlled conditions (Table S1).

Physiological assessment

The maximum quantum yield of photosynthetic energy conversion (F_v/F_m) measured for all samples showed mean values of 0.71 (SD = ± 0.1, Fig. S1A). Measures of thalli length showed mean values of 16.6 cm (SD = ± 3.4, Fig. S1B). For these two parameters, three-way ANOVA tests did not show any significant change whatever the conditions (sampling time, temperature, or irradiance) whether considered independently or interacting (p-values > 0.05). As a proxy of the light limitation stress for the seaweed, variations in the relative concentrations of mannitol (Fig. S1C) revealed a significant interaction between time and irradiance factors (three-way ANOVA tests, Table S2). However, no significant differences in the relative concentration of mannitol were observed when comparing the sampling times, each other according to the multivariate pairwise results (Fig. S1C). Moreover, no visible evidence of thalli deterioration (e.g., bleaching or fragmentation) was observed throughout the time of the whole experiment.

Flow cytometry analyses

Abundances of heteroprokaryotic cells at the surface of *T. atomaria* were estimated through flow cytometry and revealed densities ranging from 1.2×10^5 to 1.8×10^7 cells.cm^{-2} (Fig. S2). When comparing samples over time, a significant increase was observed from field to t_2 and then t_3 samples (Table S2, Fig. S2). However, no significant difference in cell densities were observed between the different irradiance and temperature conditions (Table S2). No significant factors interactions were also observed when considering the possible combinations between time, temperature, and irradiance conditions (Table S2).

Epibacterial community diversity

NOCHL primers were recently designed for studies on algal-associated bacterial communities, to avoid the contamination of 16S rRNA gene sequences from plastids (Thomas et al., 2020). In this study, this combination was firstly compared to 515F-Y/926R primers, leading to similar patterns of community structure (Fig. S3, details in SI, Mantel test at the order level: $p = 0.001$, $r = 0.8$). NOCHL were chosen because no chloroplast 16S rRNA gene sequence was obtained, which could have been a particular issue in this study due to the high number of sporophytes noticed at the algae surface (details in SI).

While no difference appeared between field and t_0 samples, a global increase of the Shannon index was observed over time from t_0 to t_3 (Fig. S4). More precisely, t_0 and t_1 samples exhibited a significantly lower α-diversity in comparison with t_2 and t_3 samples. Moreover, at t_3 and for AI, Shannon index showed significant lower values for samples at HT (Fig. S4, Table S2). Chao1 values for field samples were significantly lower than those of all the controlled conditions samples (Fig. S4, Table S2). At t_3, whatever the irradiance condition, Chao1 showed significant lower values for HT samples compared to those at AT. At AI and HI, HT samples showed also lower values than those of LT samples (Fig. S4, Table S2). No significant factor interactions were observed between time, temperature and irradiance for both α-diversity indexes (Table S2).

Considering the β-diversity, the first axis of the weighted-Unifrac based NMDS revealed a global shift from field to controlled conditions samples, despite a relatively high heterogeneity among controlled conditions samples (Fig. 2A). Moreover, a shift of the prokaryotic community was

observed on the same axis over time from t_1 to t_3 samples (PERMANOVA test using the time factor: $p = 0.001$, Table S3). The corresponding multivariate pairwise test showed that field, t_1, t_2 and t_3 samples appeared significantly different from each other while t_0 samples were not differentiated from field and t_1 ones (Table S4). On the second axis of the NMDS, differences appeared according to temperatures with a cluster of HT samples distinct from AT and LT samples (Fig. S5A, PERMANOVA test using the "Temperature" factor: $p = 0.001$, Table S3). A significant interaction between time and temperature was also observed according to the PERMANOVA test (Table S3). The three conditions (LT, AT and HT) appeared significantly distinct from each other when compared with a multivariate pairwise test (Table S4). For irradiance, HI samples were significantly differentiated from AI and LI ones, while no differences were observed between the two latter groups. When considering t_1, t_2, or t_3 samples independently (Fig. 3), the resulting NMDS plots showed separated clusters for each temperature (PERMANOVA and pairwise tests: $p = 0.001$, Tables S3 and S4). However, no significant differences were observed within the three irradiances for t_1 or t_2 samples (Table S4). Finally, t_3 samples were discriminated according to irradiance as HI and LI samples were significantly different (Table S3 and S4).

A Venn diagram (Fig. S6) revealed that the percentage of OTUs and sequences shared between all samples (field and controlled conditions samples) reached 53.8 and 88.7%, respectively. The percentages of OTUs and sequences common to only controlled conditions samples (t_0, t_1, t_2 and t_3) corresponded to 20 and 8.3%, respectively.

Considering the taxonomic affiliation of the epibacterial community, differences between field and controlled conditions samples were observed at the family level, (Fig. S7). In field samples, the main families observed were Hyphomonadaceae (Alphaproteobacteria), Alteromonadaceae, Thiohalorbdaceae (Gammaproteobacteria) and Saprospiraceae (Bacteroidetes) representing 21, 15, 15 and 14 % of the community, respectively. Hyphomonadaceae appeared as a discriminant taxon of field samples (LDA > 4, Table S5). Thioharlobdaceae and Hyphomonadaceae were mainly represented by the genera *Granulosicoccus* and *Litorimonas* contributing up to 8 and 6% to the dissimilarity between field and t_0 samples, respectively (Table S6).

In contrast, the community structure of controlled conditions samples was mainly characterized by the occurrence of Alteromonadaceae and Rhodobacteraceae with relative percentages ranging from 9 to 61% and 9 to 44%, respectively (Fig. S7). The Alteromonadaceae family appeared mainly represented by the genera *Alteromonas* and *Paraglaciecola* which were discriminant taxa specific to t_0 samples (Table S5) and contributed to 13 and 3% of the overall dissimilarity between field and t_0 samples, respectively (Tables S6).

From t_0 to t_3, and whatever the temperature/irradiance conditions, a clear decrease of Alteromonadaceae and an increase of Spongiibacteraceae, Rhizobiaceae (mainly represented by the genus *Lentilitoribacter*) and Cellvibrionaceae was noticed (Fig. S7). These three latter families appeared as discriminant taxa specific to t_3 samples (LDA > 4, Table S5).

For the analysis of discriminant taxa, a focus was made on t_3 samples since it was expected to offer the most marked differences in line with the changing conditions (Table S7 ; Fig. 4 ; Fig. S8). Actually, the highest number of discriminant taxa of a specific irradiance/temperature condition for a same LDA threshold was observed for t_3, whatever the taxonomical rank. More precisely, for thresholds of 3.4 and above, t_3 samples gathered approximately two and four times more discriminant genera than t_2 and t_1 samples, respectively. Overall, discriminant taxa specific of t_3 samples mostly differed according to the temperature (Fig. 4). The genus *Oleiphilus* occurred mainly among LT samples, whatever the irradiance, and appeared as an example of taxa displaying a similar trend for t_1 and t_2 samples (Fig. S8). Several other genera showed a similar tendency under particular conditions of irradiance, such as *Kordia* at AI and *Neptuniibacter* at LI. In contrast, some genera occurred mainly in samples at HT, such as *Sulfitobacter*, *Congregibacter* and *Parvularcula* at AI, *Hirschia* at LI, *Congregibacter* and *Parvularcula* at HI. Moreover, some genera also differed according to the irradiance conditions, such as *Kordia* at LT which occurred mainly at AI compared to LI and HI. At HT, *Lentilitoribacter* and *Parvularcula* were found in significantly higher percentages at HI compared to LI. A similar tendency was observed for samples subjected to AT for the genus *Jannaschia*.

Surface metabolome fingerprinting and variations of discriminant metabolites

When all samples were included, differences of surface metabolome profiles between field and controlled conditions samples appeared on the second component of the PCA score plot (Fig. 2B). Moreover, a global shift of the surface metabolomes was observed over time on the first component from t_1 to t_3. Finally, a discrimination was also observed on the second component of the PCA between HI and LI samples (Fig. S5B). The PERMANOVA test conducted with the three experimental factors (time, temperature, and irradiance) validated significant differences within each factor, but also a significant interactive effect of the three factors (Table S8). The multivariate pairwise analysis revealed at first that all sampling times were significantly different from each other except t_3 with field, t_0 and t_2 on one hand, and t_1 with t_0 on the other hand (Table S9). When comparing the three groups of samples obtained with different irradiances, all of them were significantly different from each other, while for temperature conditions, HT samples were significantly discriminated from AT and LT samples on the basis of their surface metabolome.

The PCA plot obtained only with the t_1 samples did not reveal any clear differences between the temperature/irradiance conditions (Fig. 5). However, multivariate tests showed that LI and HI samples were statistically different (Table S9). In the case of t_2 samples, the resulting PCA plot (Fig. 5) allowed to discriminate: (i) HT samples from the two other temperature conditions on the first component, (ii) on the second component, LI from HI samples (PERMANOVA tests with "temperature" or "irradiance" factors: $p = 0.001$, Table S8). Pairwise comparisons showed significant differences between HT samples and those at the two other temperatures on one hand, and between LI samples and those obtained at the two other irradiances on the other hand (Table S9). Finally, the corresponding PCA plot (Fig. 5) for t_3 samples showed a discrimination between HI and LI samples on one hand, and between HT and LT samples on the other hand. In term of pairwise comparisons, samples were significantly different between each temperature (Tables S9). LI samples appeared also significantly different from samples obtained at the two other irradiances (Table S9). Moreover, the interaction of temperature and irradiance was found to be significant only for t_3, in contrast to the two previous sampling times (Table S8).

When comparing field and t_0 samples, the most discriminant compounds identified according to their Variable Importance in Projection (VIP) scores were fucoxanthin (VIP score: 1.87) and

phenylalanine (VIP score: 1.85). These two compounds were more produced in t_0 samples compared to field samples (Fig. S9) with a fold change of 7.0 and 6.2, respectively.

Subsequently, a focus was made on the variations of a panel of annotated and discriminant surface compounds (Fig. 6; Fig. S9; Table S10) differentially expressed in t_3 samples according to each condition (VIP score > 0.6), since this sampling time offered the largest number of significant and discriminant variations. Such variations were not systematically observed in samples collected at previous sampling times (Fig. S9).

At LT, DMSP, mannitol, several diacylglycerylhydroxymethyl-*N*,*N*,*N*-trimethyl-β-alanine (DGTAs) [such as DGTA (C42:11), DGTA (C40:8), DGTA (C36:4) and DGTA (C36:9)] and a diacylglycerol [DG (C36:9)] were found in higher concentrations in HI samples compared to those at LI. Moreover, mannitol and DGTA (C36:4) were also more produced in AI compared to LI, while DGTA (C42:11) and DG (C36:9) were found in higher concentrations at HI rather than AI. At AT, mannitol was found in higher amounts at AI and HI rather than at LI and gleenol was also found in higher concentrations in AI rather than at LI. A quite opposite tendency was observed for fucoxanthin which appeared in higher amounts in samples at LI compared to those obtained at HI. At HT, fucoxanthin, tryptophan and an unknown sesquiterpene with the molecular formula $C_{15}H_{18}O_2$ were produced in lower concentrations in samples at LI rather than those at HI while the opposite tendency was observed for mannitol.

At LI, DGTA (C36:4), gleenol and phenylalanine were more produced in HT samples rather than those at LT. At AI, proline betaine and DG (C36:9) were found in higher concentrations in LT samples compared to HT ones. DG (C36:9) was also more produced in samples at LT compared to those obtained at AT. Gleenol was found in higher concentrations at AT than at HT. At HI, DGTA (C42:11) and DGTA (C36:0) were produced in higher concentrations in LT samples compared to AT and HT samples.

Discussion

In a general context of global change, the impact of environmental factors on the surface microbiota of marine holobionts is still poorly studied through controlled conditions experiments and the combination with the surface host's metabolome characterization remains rare. In the

case of *T. atomaria*, the concurrent temporal increase of temperature and irradiance has been hypothesized to play a key role in controlling seaweed-microbiota interactions in natural environment (Paix et al., 2019, Paix et al., *in prep.*), while a decrease of these parameters had been never investigated before. The aim of this study was to decouple these two factors to understand their specific and synergistic effects on the host-surface microbiota interactions.

Through this study, we also aimed to confirm the efficiency of NOCHL primers to avoid plastid 16S rRNA gene amplification. Their amplification led to a decrease of the sequencing depth for prokaryotic 16S rRNA sequences which can prevent a full assessment of the diversity of prokaryotic communities associated to plants or algae. We compared this set of primers with 515F-Y/926R primers which previously lead up to 36% of chloroplast 16S rRNA gene sequences (Paix et al., 2020). We confirmed the results from Thomas et al., 2020, since the efficiency of NOCHL primers was clearly observed with no sequences affiliated to chloroplasts.

Conditioning effect on the holobiont system

Heteroprokaryotic densities and richness of the epiphytic community appeared higher for controlled conditions samples after the one-week acclimation period compared to field ones. A difference in β-diversity was also observed between these two sets of samples. Besides, a relatively high percentage of OTUs number (20%) were specific to controlled conditions samples. However, these specific OTUs represented a lower proportion in terms of sequences (8.3%), compared to their percentage based on the number of OTUs. Two plausible scenarios could explain the presence of such epibionts at the surface of controlled conditions samples despite they had not been observed within field samples. Firstly, these OTUs could be rare taxa in field samples, removed with the 0.005% filtering process of the FROGS pipeline (used for filtering the sequencing artefacts, Bokulich et al., 2013) or with the rarefaction of the OTU-table. These taxa may benefit from the algal conditioning and become more abundant at the algal surface in aquaria. Another source could be the pre-filtration process of the running seawater. Once pretreated, the running coastal seawater provided to the aquarium device was filtered (with ultimately 1 to 3 μm filters) and then sterilized using UV radiations. However, despite these filtration steps, some exogenous colonizers might come from the planktonic community from the coastal sea, or also from biofilms on the surfaces of the experimental devices (e.g. tubes or filters).

Considering these two scenarios, it cannot be excluded that these rare or/and exogenous taxa may also benefit from the change of uncontrolled and/or not measured parameters throughout the experiment. Such hypothesis might explain the significant interaction observed between time and temperature factors and could be considered as a limitation for this study, raising the importance of monitoring a large panel of environmental parameters to adjust and improve the stability of the experimental setup.

The effect of a controlled conditioning on the surface microbiota was already investigated for the Rhodophyta *Delisea pulchra* and a similar scenario was also proposed by the authors (Zozaya-Valdés et al., 2016). 15 days after the transfer of *D. pulchra* from field to aquaria, a change of microbiota structure was observed with specific enriched OTUs. The main ones were affiliated to Kordiimonadales (mainly the genus *Kordiimonas*), Alteromonadales (mainly the genus *Glaciecola*) and Cytophagales. In our study, the main taxa promoted after one week of acclimation also belonged to Alteromonadales with the genera *Alteromonas* and *Paraglaciecola*. Several strains belonging to these two genera have been previously described for their ability to degrade seaweed polysaccharides (Akagawa-Matsushita et al., 1992; Schultz-Johansen et al., 2016; Bech et al., 2017). Moreover, the genus *Alteromonas* was already identified as increasing during mesocosm experiments (Schäfer et al., 2000). *Alteromonas macleodii* in particular is well known as a r-strategist, possibly taking advantage of nutrient-enriched environments (Zemb et al., 2010; Romera-Castillo et al., 2011; Tada et al., 2011; Lawes et al., 2016). Despite we used a metabolomics approach which did not allowed to investigate algal polysaccharides, we hypothesized that a shift of the global chemical composition at the algal surface (e.g. an increase of polysaccharides biosynthesis) after the conditioning might constitute a selective advantage for *Alteromonas* and *Paraglaciecola* spp., which could metabolize such a carbon source and quickly grow at the surface of *T. atomaria*.

In contrast, two other genera of the Alteromonadales, *Litorimonas* and *Granulosicoccus* spp. significantly decreased when algal samples were transferred in aquaria. These two genera have been already described at the surface of *T. atomaria* as specific, core and pioneer taxa and are known to quickly decrease over time on Mediterranean sites (Paix et al., 2019, 2020, Paix et al., *submitted*). Even if environmental conditions from the sampling site of this study clearly differ

from those of the Mediterranean ones, these taxa could be sensitive to environmental changes. Among changes mediated by the conditioning from field to mesocosms, decrease of hydrodynamics and modification of the selective pressure associated to predation or viral lysis might constitute crucial factors (Cram et al., 2016).

For the surface metabolome, several metabolites were differentially produced after the transfer of *T. atomaria* from field to aquaria. For example, phenylalanine and fucoxanthin were observed with higher concentrations after the transfer in aquaria while field samples were characterized by a higher expression of DGTAs. Within diverse algal species, phenylalanine and fucoxanthin production is known to increase with higher UV-B radiations (Heo and Jeon, 2009; Hartmann et al., 2015). Hence, the metabolomics shift linked to the transfer of *T. atomaria* from field to aquaria, might be explained by a change of light conditions/quality associated to the LED/filter system. As hypothesized for polysaccharides, such chemical variations at the algal surface might also be considered as potential factors shaping differences of epibacterial composition.

Finally, the physiological assessment of the macroalgae was more generally determine through analyses of the algal growth, the relative concentration of mannitol, and the maximum quantum yield of PSII (F_v/F_m). Linked to the algal photosynthetic activity, these two latter parameters aimed to decipher the light limitation of CO_2 fixation, and the photosynthetic efficiency of the seaweed. The variations of the mannitol concentrations during the experiment suggested that photosynthetic CO_2 fixation appeared mainly linked to irradiance level during the experiment and was limited according to the sampling times when compared independently. Moreover, F_v/F_m values did not changed significantly whatever the factors considered. Similarly, the algal growth assessed through the measurement of thalli samples, did not showed any significant differences neither with time, irradiance, or temperature conditions. Hence, regardless of conditions of irradiance and temperature, these results suggested a relative stable physiological status of the seaweed throughout the experiment.

Short-term responses of algal surface microbiota and metabolome

Through multivariate analyses conducted within t_1 samples, the short-term responses (24h) of the surface microbiota and metabolome were found to clearly differ. On one hand, short-term

differences of prokaryotic β-diversity only appeared with the change of temperature (increase and decrease). More particularly, the *Oleiphilus* genus was a major discriminant taxon which differed after t_1, with higher percentages at LT compared to AT and HT. Conversely, the absence of a direct effect of irradiance on the global structure of the bacterial community at t_1 could be linked to the absence of major phototrophic taxa in the initial community. The NOCHL primers did not allow to amplify sequences of 16S rRNA gene from Cyanobacteria (Thomas et al., 2020). However, Cyanobacteria sequences constituted less than 0.1% of the overall community for samples tested (t_0 and t_1) with the 515F-Y/926R primers. Moreover, when focusing on aerobic anoxygenic phototrophs [AAP, a functional group gathering various subgroups within Alpha-, Beta- and Gammaproteobacteria, composed of facultative photoheterotrophs which use bacteriochlorophyll to harvest light energy (Koblížek, 2015)], the main genera identified in the dataset were *Roseobacter*, *Congregibacter*, *Erythrobacter* and *Jannaschia*, but these genera represented less than 0.01% of all the sequences and did not vary significantly according to irradiance conditions in t_1 samples. Moreover, the absence of a direct effect of irradiance changes at t_1 on the epibacterial community could be explained by the fact that the growth of these main phototrophic taxa would require a longer period (e.g. one week or more, see the next section below on long-term effects).

On the other hand, short term differences between surface metabolomes were observed only when the irradiance conditions varied. The highest irradiance rapidly induced an increase of the production of mannitol at the algal surface. This polyol is a photosynthetic product which constitutes the main form of energy storage for brown algae (Lehvo et al., 2001; Rousvoal et al., 2011; Weinberger et al., 2011) and a similar observation has previously been made for *F. vesiculosus* (Saha et al., 2014).

Interestingly, these results indicated that the short-term responses of the two components of the holobiont system are not susceptible to the same factor. Consequently, we hypothesized this change of algal host and surface microbiota would correspond to responses firstly inherent to their respective physiological specificities, and that reciprocal interactions at the holobiont scale could only occur later. An interesting approach to confirm that irradiance could constitute a primary and direct parameter acting on the algal host, in contrast to the temperature, would be

to work on similar experiments with an axenic host as suggested by van der Loos et al., 2019. Despite the methodological complexity of cultivating such a model, this type of study would allow to decouple factors effects on the host without the risk that epibiotic bacterial metabolites interfere.

Effect of irradiance on surface microbiota: an indirect long-term effect mediated by the algal host?

After the conditioning, differences appeared only after two weeks between samples exposed to HI and LI, and this even more in the case of HT. The genera *Lentilitoribacter*, *Parvularcula*, *Congregibacter* (at HT), and *Jannaschia* (at AT) constituted taxa which seemed to be especially adapted to higher irradiance. *Pelagimonas* and *Kordia* were genera especially adapted to AI conditions in the case of HT and LT, respectively. The case of *Jannaschia* and *Congregibacter* is interesting since one species is known to produce the bacteriochlorophyll *a* pigment and is described as an AAP (Fuchs et al., 2007; Yoon et al., 2010; Pujalte et al., 2014; Selyanin et al., 2016). Higher irradiances could have constituted a beneficial condition thanks to its phototrophic metabolism, and the delayed response is consistent with clear effects of light observed on natural AAP communities in the long terms (Koblížek, 2015). As no evidence of phototrophic metabolism was observed for *Parvularcula*, *Pelagimonas* and *Kordia*, irradiance could then constitute an indirect factor explaining the selection of these taxa. Moreover, it was clearly established that surface metabolome was directly impacted by the irradiance changes during the whole experiment. Consequently, several surface algal metabolites differentially expressed according to light intensity could be considered as potential factors shaping microbiota light-dependent differences with time.

After two weeks, mannitol, fucoxanthin and DMSP were the main metabolites involved in the surface metabolome changes in connection with irradiance conditions. As already observed after one day, mannitol remained discriminant but with increasing concentrations in the case of HI, which may still result from a higher algal photosynthetic activity. Mannitol constitutes a preferential source of carbon for a large bacterial diversity but it is also a compatible solute known to play a role in osmoprotection (Kets et al., 1996; Sand et al., 2013; Zahid et al., 2015). Mannitol catabolism has been notably investigated through a genomic approach with *Zobellia galactanivorans*, a Flavobacteriia closely associated to several macroalgae (Barbeyron et al.,

2001; Groisillier et al., 2015). The operon associated to mannitol assimilation for this bacterial strain has been identified and also found in other genomes among Flavobacteriaceae (Groisillier et al., 2015). Interestingly, this bacteria has the ability to degrade various algal polysaccharides such as alginates and fucans of Ochrophyta, or agars and carrageenans of Rhodophyta (Thomas et al., 2012, 2013; Barbeyron et al., 2016). In addition to mannitol, algal polysaccharides could also constitute an important source of carbon for epiphytic bacteria particularly adapted to macroalgal niches (Gobet et al., 2018). Consequently, such primary or secondary products of the algal photosynthesis could then be considered as key factors involved in epibacterial communities shaping, especially in the case of changing irradiance. An interesting perspective would be to investigate the polysaccharide production of *T. atomaria*, notably under distinct irradiances and to focus on microbial functions associated with the degradation of such biopolymers.

For fucoxanthin, a higher expression was observed in the case of a LI. Increasing amounts of this carotenoid have been observed with depth or shade increase in other macroalgae such as *F. vesiculosus*, *Ascophyllum nodosum*, *Udotea petiolate*, and *Dictyota dichotoma*. These data illustrating the adaptation of the photosynthetic performances of seaweeds with a lower quantity and quality of light (Ramus et al., 1977; Perez-Bermudez et al., 1981). Here, we suggested that a similar shade-light adaptation occurred in *T. atomaria* to compensate the irradiance decrease. Through culture dependent approaches, fucoxanthin was also found to display inhibiting activities against bacterial adhesion (Viano et al., 2009; Saha et al., 2011). However, the selective effect of fucoxanthin on the epibacterial community structure of macroalgae is always a matter of discussion (Lachnit et al., 2010; Saha et al., 2011; Egan et al., 2013). In Saha et al., 2014, correlations between fucoxanthin and several bacterial taxa were investigated and several "fucoxanthin-positive" and "-negative" taxa have been determined. The Flavobacteriaceae family was notably found positively correlated to fucoxanthin suggesting that members of this family could be attracted by this compound. Here, no clear correlation was observed between Flavobacteriaceae and fucoxanthin (linear regression: $R^2 < 0.2$). Through *in vitro* and *in vivo* field experimental approaches, the anti-adhesion activity of fucoxanthin and of potentially unidentified compounds of a non-polar fraction of the surface extracts of *F. vesiculosus*, has been previously supported. However, fucoxanthin has not been found to impact the community

488 structure of *F. vesiculosus* and cautions have been raised to avoid any premature causality links
489 (Lachnit et al., 2013). A low selective range of activity may be important to consider (Egan et al.,
490 2013) and further investigations still need to be conducted to clearly understand the effect of
491 fucoxanthin on macroalgal epibacterial communities under ecological relevant conditions.

492 In a previous work on Mediterranean samples of *T. atomaria*, DMSP was found to increase at the
493 algal surface from February to July and such a variation was hypothesized to be correlated with
494 the temporal increase of temperature and/or irradiance (Paix et al., 2019). In the present study,
495 DMSP increased significantly with the irradiance intensity in the case of LT conditions. The DMSP
496 concentrations of total extracts have been previously investigated under different light conditions
497 in other seaweeds, such as the green algae *Ulothrix implexa, Ulothrix subflaccida, Enteromorpha*
498 *bulbosa*, *Acrosiphonia arcta*, *Ulva rigida*, *Blidingia minima* (Karsten et al., 1990, 1992)*, Ulva*
499 *lactuca* (Van Alstyne and Puglisi, 2007), *Codium fragile* (Lyons et al., 2010) and the brown alga *F.*
500 *vesiculosus* (Saha et al., 2014). In accordance with our results, Karsten et al., 1990, 1992 and Lyons
501 et al., 2010, have found in their respective algal models that DMSP concentrations were higher
502 with an increasing irradiance. Taken together, these results may strengthen the hypothesis of a
503 light-dependent DMSP biosynthesis, especially in the case of low temperature conditions (Karsten
504 et al., 1992). Moreover, DMSP is also produced by many microalgae, including dinoflagellates and
505 diatoms (Bullock et al., 2017), and the potential origin of DMSP at the surface of *T. atomaria* could
506 also be linked to such epiphytes that were identified on several Dictyotaceae including *T.*
507 *atomaria* (Ternon et al., 2020). Besides, DMSP constitutes a source of carbon and sulfur for a large
508 diversity of bacteria, especially those from the *Roseobacter* clade (Howard et al., 2008; Curson et
509 al., 2011; Dogs et al., 2017). DMSP is also known as a chemo-attracting compound released at the
510 surface of *Ulva mutabilis* which allows the "gardening" and mutualistic interactions with
511 *Roseovarius* sp. (Wichard et al., 2015; Kessler et al., 2018). At the surface of *T. atomaria*, several
512 discriminant taxa such as *Sulfitobacter* and *Jannaschia*, specific to a condition of temperature and
513 irradiance at t_3, have been already described for their DMSP catabolic activity (Mou et al., 2005;
514 Curson et al., 2008; Howard et al., 2008). More precisely, an interactive effect of temperature and
515 irradiance was observed for the genus *Jannaschia*, with a maximum abundance under HI and AT
516 conditions as mentioned above. Then, the higher DMSP production induced by a higher irradiance

517 could also positively affect the growth and development of members of this genus at the surface
518 of *T. atomaria*.

519 ## Effect of temperature on the holobiont dynamics

520 The increase of seawater temperature was predicted to potentially affect macroalgae health at a
521 global scale (Egan and Gardiner, 2016; Bindoff et al., 2019; van der Loos et al., 2019). At the
522 holobiont scale, temperature affects microbial shifts for a large number of seaweeds in controlled
523 condition studies, such as *D. pulchra* from the Tasman sea (Zozaya-Valdés et al., 2016),
524 *Neogoniolithon fosliei* from the Coral sea (Webster et al., 2011), *Macrocystis pyrifera* from NE
525 Pacific coasts (Minich et al., 2018), *Amphiroa gracilis* from the SE Indian ocean (Huggett et al.,
526 2018), *Fucus vesiculosus f. mytili* from the North sea (Mensch et al., 2016) and *F. vesiculosus* from
527 the Baltic sea (Stratil et al., 2013). Concerns are notably raised since lower health conditions and
528 chemical defenses caused by increasing temperature can result to a microbiota dysbiosis (Egan
529 et al., 2014; Egan and Gardiner, 2016; Minich et al., 2018). More precisely, the development of
530 opportunistic pathogens could be promoted through the activation of virulence factors (Case et
531 al., 2011; Fernandes et al., 2011; Gardiner et al., 2017).

532 Among epiphytic bacteria which are known to be favored by an increase of seawater
533 temperature, the Rhodobacteraceae family is particularly represented (Case et al., 2011;
534 Fernandes et al., 2011; Stratil et al., 2013; Saha et al., 2014; Qiu et al., 2019). In the case of *D.*
535 *pulchra*, pathogens from the Roseobacter group have been particularly observed, especially for
536 bleached algae under high temperature conditions (Case et al., 2011; Zozaya-Valdés et al., 2015,
537 2016). However, pathogens of *D. pulchra* are not specifically restricted to this family (Kumar et
538 al., 2016). In the present study, Rhodobacteraceae family appeared to be the main family
539 increasing with the temperature, with notably the genus *Sulfitobacter*. Interestingly, the genus
540 *Sulfitobacter* was also found to be positively correlated to the temperature at the surface of *M.*
541 *pyrifera* harvested[BP1][c2] on the Chilean coasts (Florez et al., 2019). Attention was also paid on
542 variations of several taxa from this family known as potential pathogens, such as *Nautella*,
543 *Phaeobacter* and *Aquimarina* (Fernandes et al., 2011; Kumar et al., 2016). The contribution of
544 these potential pathogens to the overall microbiota shift in response to an increase of

545 temperature was not significant. Moreover, no clear disease event (bleaching, blistered or
546 disrupted tissues) was observed on thalli of *T. atomaria* during the whole study.

547 However, a lower α-diversity in terms of richness, was observed when temperature increases.
548 Considering that a decrease of richness but not diversity (in HI and LI conditions) might indicate a
549 loss of "rare" taxa, this change of α-diversity could constitute a transient phase before a newly
550 more diversified and stable state.

551 However, in the case of human holobiont, a decrease of α-diversity constitutes a sign of a
552 potential dysbiosis (Pitlik and Koren, 2017). For marine holobionts, including seaweeds, a high
553 diversity is often considered to be essential for the stability and the resilience of the holobiont
554 system under changing conditions (Loreau et al., 2001; Moore, 2005; Longford et al., 2019).
555 Consequently, even if no clear pathogens were identified at the surface of *T. atomaria*, a
556 decreasing richness under higher temperatures may suggest a lower fitness of the holobiont.

557 A global shift of the β-diversity of the surface microbiota of *T. atomaria* was observed after one
558 day under high temperature conditions while modifications of the surface metabolome were only
559 observed after one week. For the β-diversity, significant interactions were observed between
560 time and temperature, suggesting a continuous shift toward a stable structure occurring after a
561 long-term period. For the metabolome, significant interactions between temperature and
562 irradiance were observed only at t_3. We hypothesized that temperature may directly modify the
563 microbiota community structure over time and later induce an adaptive response of the algal
564 metabolome which in turn regulate the epibiosis. In Othmani et al., 2016, the anti-adhesion
565 activity of several sesquiterpenes found at the surface of *T. atomaria* has been investigated
566 against several bacterial strains isolated from marine biofilms. The gleenol, a spiroaxane
567 sesquiterpene, has shown strong anti-adhesion activities at relevant natural concentrations. This
568 compound has been proposed to play an important role on the chemical selection of a specific
569 microbial community at the surface of *T. atomaria* (Othmani et al., 2016). In the present study,
570 the amounts of gleenol at the algal surface appeared to reach their maximal level at HT/LI and
571 AT/AI for t_3 samples. The differential production of this metabolite could possibly constitute a

host adaptation to limit quantitatively and/or qualitatively the dynamics of the microbiota composition induced by the change of temperature.

Changes of the surface metabolome of *T. atomaria* linked to temperature variations could also be attributed directly to physiological processes inherent to the algal host. Among other metabolites which differ significantly according to temperature, several polyunsaturated membrane lipids were identified, including diacylglycerols (DGs) and DGTAs. These lipids were mainly expressed in the case of LT. Here, we hypothesized that thalli of *T. atomaria* exposed to HT express less polyunsaturated lipids in order to decrease the fluidity of its membrane. Such changes in membrane lipid composition for seaweeds has been already described as a mean to maintain an optimal membrane fluidity under changing temperature conditions (Eggert, 2012). Besides, this process is also well known in the case of microalgae (Sato and Murata, 1980, 1982; Schüler et al., 2017). This adaptation to temperature change could thus play a crucial role to maintain the integrity of several membrane process, including enzymatic mechanisms such as the induction of heat-shock genes during the membrane rigidification of *Synechocystis* (Inaba et al., 2003; Los and Murata, 2004; Eggert, 2012).

Conclusion

To our knowledge, this is the first multi-omics study, coupling untargeted metabolomics and 16S rRNA gene metabarcoding, to study a seaweed holobiont responses to experimentally controlled environmental conditions. Through such anapproach, we showed that the seaweed-holobiont dynamics of the Phaeophyceae *T. atomaria* was shaped by both temperature and irradiance. The response to temperature changes appeared to be faster for the microbiota than for the metabolome at the surface of the alga. Conversely, irradiance changes may impact firstly the algal surface metabolome and, only then, its associated microbiota. We suggested that indirect effects could occur only after few days. Algal metabolome variations resulting from a differential photosynthetic activity induced by a shift of irradiance could be a factor shaping thereafter the epiphytic microbiota. Several metabolites, such as mannitol, fucoxanthin and DMSP, known to play important roles on seaweed-microbiota interactions could be involved. Overall, bacterial richness appeared lower in the case of a higher temperature with a positive selection of several specific taxa (notably from the Rhodobacteraceae family), probably taking advantage over other

601 families (such as Oleiphilaceae and Flavobacteriaceae, mainly represented by the genera
602 *Oleiphilus* and *Kordia*, respectively). These results suggested to better investigate the algal fitness
603 in future studies.

Experimental procedures

Aquarium experimental device

The whole experimental device was set up at the "Roscoff Aquarium Services" structure (Centre de Ressources Biologiques Marines, Station Biologique de Roscoff, France) in a thermostated room at 16°C. The room had three shelves, each of them with three floors. Each floor gathered three replicate aquaria (15L each), resulting in a total of 27 aquaria (Fig. S10 and S11). Each shelves system was supplied by the same independent semi-open water circuit with pre-treated running seawater pumped from Roscoff coasts [details of pre-treatment in Supplementary information (SI)]. At first, the pre-treated seawater went through an independent 50L tank for each shelf and was UV-treated with a Reeflex UV 800 system (Eheim, Deiziau, Germany). The water temperature within each tank was conditioned by TK500/TR10 chiller/heater systems (TECO refrigeration technologies, Ravenna, Italy). Seawater was then distributed to each aquarium through a Compacton 2100 pump (Eheim). When arriving to aquaria, the mean water flow was 36.5 L h^{-1} (SD = ±7.5). Finally, the water from each aquarium went back by overflowing to the first tank through a micron bag (100 μm; Red Sea, Düsseldorf, Germany). Two rows of 12V LED ribbons (LED 5050, Inovatlantic, Nantes, France) were set up on the top of each floor resulting in an irradiance of 120 μmol photons m^{-2} s^{-1} measured at the bottom of each aquarium (SD = ±8.1). This irradiance intensity corresponds approximatively to the mean *in situ* irradiance going up to 5m depth on NW French Atlantic coasts in summer (Martin et al., 2006). Each light system was set on a 16h:8h light:dark cycle during the whole experiment, which corresponds to the natural day:night cycle at that time. To avoid any position bias between aquaria, particular cautions were taken when LED ribbons were set up, to ensure a homogenous irradiance intensity for each replicate of aquarium within the floors, during the whole experiment (SD < 9%). Additionally, external source of irradiance or heat from the thermostated room were avoided by keeping the room in the dark and each floor closed by a specific door.

Sampling and biological material

Approximatively 120 thalli of *Taonia atomaria* (Woodward) J. Agardh (Dictyotaceae, Phaeophyceae) were collected by diving at Guimaëc (The Channel, 48°41'39.9"N 3°41'50.7"W) in

July 2018 at low tide (2 to 4m depth). Thalli were stored in cool boxes filled with surrounding seawater and transported at lab within one hour after sampling.

Once at lab, only thalli with a length between 20 and 30 cm were kept considering only individuals within the same development period. Furthermore, thalli showing evidence of macrofouling at their surface were not considered and ultimately a total of 87 thalli were kept. Among them, three thalli haphazardly selected were considered as triplicates of field samples and directly used for cytometry, metabarcoding and metabolomics analyses.

Controlled conditions experiment

The 84 remaining thalli were haphazardly selected and distributed in the 27 aquaria as described in Fig. 1. The whole study was conducted with triplicates of aquaria for each condition. For each thallus, holdfasts were carefully attached to stainless steel screws in order to ballast the thallus at the bottom of the aquarium. The seawater temperature and the irradiance intensity in all aquaria were set to field conditions at 18°C (SD = ± 0.2) and 120 μmol photons m^{-2} s^{-1} (SD = ± 10.5), respectively, and used for an acclimation period of one week. At the end of the acclimation (t_0), three replicates were sampled (t_0 samples, Fig. 1) and analyzed. After this sampling, all the aquaria contained three thalli (on for each following sampling times) and the conditioning period was started with 9 distinct conditions: three temperature coupled with three irradiances. The three chiller/heater systems from each shelf were set to 13°C (SD = ± 0.6), kept to 18°C (SD = ± 0.2) or set to 22°C (SD = ± 0.5). These “low”, “ambient” and “high” temperature conditions were named LT, AT and HT, respectively. The change of temperature was progressively done during 3h. For each floor, the irradiance of (i) bottom floors was set to 20 μmol photons m^{-2} s^{-1} (SD = ± 0.75) by adding a solar film (F339-2000 , d-c Fix®), (ii) mid floors was kept to 120 μmol photons m^{-2} s^{-1} (SD = ± 10.5), (iii) top floors was set to 350 μmol photons m^{-2} s^{-1} (SD = ± 10.6) by turning on two supplementary LED ribbons. These “low”, “ambient” and “high” irradiances conditions were named LI, AI and HI, respectively.

One day after, one thallus per aquarium was chosen haphazardly and sampled, consisting in 27 t_1 samples (9 cross-conditions in triplicates, Fig. 1). One and two weeks after t_0, two other samplings were performed in the same way with 27 t_2 and 27 t_3 samples, respectively (Fig. 1). For all

sampling points, each replicate of sample (i.e. an individual thallus) was subjected to four types of analyses : (i) measurement of maximum quantum yield [F_v/F_m] of photosynthetic energy conversion, (ii) flow cytometry, (iii) 16S rRNA gene metabarcoding, (iv) and UHPLC metabolomics analyses, using four distinct fronds from the same thallus [average surface of a frond: 13.5 cm^2 (SD = ±7.4)].

Physicochemical parameters measurements

Temperature, irradiance, pH, salinity and dissolved O_2 level were monitored daily in each aquarium (details in SI). Concentrations of nitrates (NO_3^-), orthophosphates (PO_4^{3-}), and silicates [$Si(OH)_4$] were determined in field and aquarium seawater at each sampling time (details in SI). Measurement methods were done as described in Briand et al., 2017.

Physiological assessment

Before extraction procedures, the maximum quantum yield (F_v/F_m) of photosynthetic energy conversion of the photosystem II (PSII) of each sample was measured using a pulse-amplitude modulated chlorophyll fluorometer (JUNIOR-PAM teaching Chlorophyll Flurorometer, Walz, Germany). A frond of each replicate was kept 2 min in the dark and three measures were done by placing directly the optic fiber along three surface areas chosen haphazardly on the algal frond. The mannitol being a main primary source of energy for brown seaweeds, its concentration can be used as a proxy linked with CO_2 fixation through the seaweed photosynthesis (Saha et al., 2014). The relative concentration of this primary metabolite was determined through the metabolomics analysis (see below). The algal growth was investigated throughout the experiment by measuring the length of all thalli sampled for the cytometry, metabolomics and metabarcoding experiments, and then kept in the herbarium. Furthermore, a particular attention was paid during the whole experiment to identify any visual evidence of thallus deteriorations such as bleaching or other types of tissue degradation.

Flow cytometry analyses

Flow cytometry (FCM) analyses were used to assess the densities of heterotrophic prokaryotes at the surface of the algal samples. Epiphytic cells were collected by scraping the surface of an entire frond of each sample with a sterile scalpel, prefiltered using 40 μm cell strainers, fixed in 4 mL of

1% glutaraldehyde filtered seawater solution and conserved at -80°C. The other fronds of each thalli samples were kept for metabarcoding and metabolomics analyses. Aggregated cells were dissociated with an optimized sonication time of 2 min. Samples were centrifugated at 800*g* for 1 min and 200 μL of supernatant were stained using SYBR Green I (Invitrogen, Carlsbad, CA, USA). Cells were enumerated using a BD Accuri C6 flow cytometer (BD Biosciences, San Jose, CA, USA) as previously described (Paix et al., 2020). Results were expressed as densities of cells (cells.cm^{-2}) using the measured surface area of each algal sample.

16S rRNA gene metabarcoding analyses

Epiphytic cells were collected by scraping the surface of an entire frond of each sample with a sterile scalpel. DNA extraction was performed using the DNeasy PowerBiofilm kit (MoBio, Qiagen, Germantown, MD, USA) and samples were conserved at -80°C (Paix et al., 2019, 2020).

The NOCHL primers were previously designed specifically to minimize the contamination from plastid 16S rRNA gene (Thomas et al., 2020). At first, they were tested to estimate their efficiency to avoid amplification of chloroplastic 16S rRNA gene and were compared to the 515F-Y/926R primers sets (Parada et al., 2016). Both pairs of primers were tested on triplicates of t_0 and t_1 (AT/AI) samples. The treatment of sequences for these analyses with both primers pairs was performed as described below.

Following these analyses, 16S rRNA genes of all samples were amplified using the NOCHL primers. Amplicons were sent to Eurofins Genomics (Ebersberg, Germany) for MiSeq Illumina sequencing (2×300 bp). 16S rRNA gene reads were processed using the FROGS workflow under the Galaxy environment (Escudié et al., 2018). Clustering step for generating operational taxonomic units (OTUs) was performed using SWARM with a clustering aggregation distance set to 3 (Mahé et al., 2014). Chimeric sequences were *de novo* removed using VSEARCH (Rognes et al., 2016). OTUs representing less than 0.005% of all the sequences were removed. OTUs were affiliated with the silva132 16S rRNA gene database. The final matrix was obtained by performing a rarefaction to the minimum library size (21 642 reads) using the "phyloseq" R package (McMurdie and Holmes, 2013).

α-diversity was estimated using Chao1 and Shannon indexes. β-diversity was analyzed with a non-metric multidimensional scaling (NMDS) using weighted UniFrac distances allowing to consider phylogenetic relationships between OTUs. These analyses were performed using the "phyloseq" R package and graphical outputs were generated using the "ggplot2" R package.

A Venn diagram was constructed to reveal percentages of OTUs and sequences shared between the samples collected at different sampling times. An OTU was considered as common to all the sampling times when it was found a least in one replicate of each sampling time. The Venn diagram was calculated with the Venn webtool (http://bioinformatics.psb.ugent.be/webtools/Venn/). LEfSe analyses were conducted to reveal discriminant taxa whether specific to a sampling time (from field to t_3 samples) or a particular controlled cross-condition (n = 9). LEfSe analyses were performed under the Galaxy environment with a LDA threshold set to 3.4. A focus on specific comparisons was made with SIMPER analyses to reveal the main contributing genera involved in the dissimilarity between field and t_0 samples. SIMPER analyses were conducted with the "vegan" R package with p values calculated through 999 permutations.

UHPLC metabolomics analyses

Extraction of surface metabolites and sample preparation were performed as described in Paix et al., 2019, 2020 (details in SI), using an entire frond of each sample. Surface extracts were analyzed using a UHPLC-ESI-HRMS system (Dionex Ultimate 3000 rapid Separation; Thermo Fisher Scientific) equipped with an analytical core-shell reversed phase column (150 × 2.1 mm, 1.7 μm, Kinetex Phenyl-Hexyl; Phenomenex, Le Pecq, France) and coupled with an ESI-QToF Impact II mass spectrometer (Bruker Daltonics, Bremen, Germany) using a positive ionization mode (details in SI).

Raw UPLC-MS data were converted into netCDF files using DataAnalysis software (v. 4.3; Bruker, Germany) and processed for peak finding, integration and alignment using MzMine 2 (version 2.53, Pluskal et al., 2010; details in SI). Data were filtered according to Favre et al., 2017, by taking into account signal/noise ratio, coefficient of variation and coefficient of correlation. The resulting data matrix (101 features) was $\log_{10}$-transformed, mean-centered, normalized using the sum of

the chromatographic peak areas according to Paix et al., 2020. The data matrix was then analyzed using principal component analysis (PCA) and partial least-square discriminant analysis (PLS-DA) to determine the chemical biomarkers of a specific condition of temperature and irradiance.

The global annotation was performed as described in Paix et al., 2019, 2020; Carriot et al., 2020. Briefly, the annotation was based on the use of an "in-house" database described in Carriot et al., 2021, gathering metabolites annotated through the use of molecular networks (details in SI). Based on the PLS-DA components, VIP scores were calculated and indicated the importance of each *m/z* feature in the discrimination between each group of samples, allowing then to identify the main biomarkers of a specific condition of temperature and irradiance. A particular attention was paid on compounds with a VIP score above 0.6 (details in SI). Thus, among the 101 features of the data matrix, the 30 metabolites with the highest VIP scores were annotated. In brief, annotation was assessed by comparison of MS/MS spectra with those of our in-house database (purified compounds and commercial standards listed in SI), and public databases such as MetLin, MoNA or Lipidmaps. To confirm the annotation, elucidation of the MS/MS fragmentation pathway was performed and when possible compared to the literature (details in SI).

Statistical tests

Three-way ANOVA tests were conducted to assess the significance of physicochemical parameters, PAM measures, metabolites, densities, according to each experimental condition (time, irradiance and temperature). ANOVA tests were followed by pairwise multiple comparison tests. Tukey's post-hoc tests were performed for PAM measures, discriminant metabolites, densities and α-diversity metrics. Duncan test with Benjamini-Hochberg method for *p*-value correction was performed as a multiple testing method to evaluate differences between groups for discriminant taxa. Following NMDS and PCA, overall differences between temperature/irradiance conditions were statistically tested with PERMANOVA and followed by a multivariate pairwise test. These analyses were conducted on R with "ade4", "agricolae", "vegan" and "RVAideMemoire" packages. PLS-DA were subjected to cross validations using MetaboAnalyst 4.0 (https://www.metaboanalyst.ca).

Acknowledgments

This work was supported by the “Sud Provence-Alpes-Côte d’Azur” regional council (B.P. PhD grant). This work was also carried out with infrastructure provided by EMBRC France (grant no. ANR-10-INBS-0002) project “EMPREINTES”. We are grateful to N. Carriot (MAPIEM, University of Toulon, France) for his help with annotation of the metabolomics data processing, to S. Greff (IMBE, Aix-Marseille University, France), to C. Leroux (Corsaire-Metabomer, FR 2424, Marine Station, France) and E. Bourrigaux (Visiting scientist facilities service, FR 2424, Roscoff Marine Station, France) for their technical supports. We acknowledge F. Thomas and A. Gobet for sharing their useful work on the NOCHL primers. We thank C. Vieira for confirming the identification of *Taonia atomaria* through phylogenetic analyses.

Data accessibility

Sequences data were deposited and are publicly available in the NCBI Sequences Read Archive (SRA) under the BioProject ID PRJNA684487 accession number. Raw data for LC-ESI-(+)-MS/MS experiments were deposited and are publicly available in the MassIVE platform under the ID MSV000084512, respectively.

Author contributions

BP, GC, JFB, CL and PP designed the study. BP and PP performed field sampling. BP and GS designed and constructed the whole experimental devices. BP performed the controlled conditions experiments, PAM measurements, metabolomics and metabarcoding experiments. BP and BM performed cytometry analyses. NL and CLP performed chemical analyses of seawater samples. BP, GC, JFB, PP and CL analyzed all the data. All authors participated to the writing of the manuscript.

References

Akagawa-Matsushita, M., Matsuo, M., Koga, Y., and Yamasato, K. (1992). *Alteromonas atlantica* sp. nov. and *Alteromonas carrageenovora* sp. nov., bacteria that decompose algal polysaccharides. *Int. J. Syst. Evol. Microbiol.* 42, 621–627. doi:10.1099/00207713-42-4-621.

Barbeyron, T., L'Haridon, S., Corre, E., Kloareg, B., and Potin, P. (2001). *Zobellia galactanovorans* gen. nov., sp. nov., a marine species of Flavobacteriaceae isolated from a red alga, and classification of [*Cytophaga*] *uliginosa* (ZoBell and Upham 1944) Reichenbach 1989 as *Zobellia uliginosa* gen. nov., comb. nov. *Int. J. Syst. Evol. Microbiol.* 51, 985–997. doi:10.1099/00207713-51-3-985.

Barbeyron, T., Thomas, F., Barbe, V., Teeling, H., Schenowitz, C., Dossat, C., et al. (2016). Habitat and taxon as driving forces of carbohydrate catabolism in marine heterotrophic bacteria: example of the model algae-associated bacterium *Zobellia galactanivorans* DsijT. *Environ. Microbiol.* 18, 4610–4627. doi:10.1111/1462-2920.13584.

Bech, P. K., Schultz-Johansen, M., Glaring, M. A., Barbeyron, T., Czjzek, M., and Stougaard, P. (2017). *Paraglaciecola hydrolytica* sp. nov., a bacterium with hydrolytic activity against multiple seaweed-derived polysaccharides. *Int. J. Syst. Evol. Microbiol.* 67, 2242–2247. doi:10.1099/ijsem.0.001933.

Bindoff, N. L., Cheung, W. W. L., Kairo, J. G., Arístegui, J., Guinder, V. A., Hallberg, R., et al. (2019). "Chapter 5: Changing ocean, marine ecosystems, and dependent communities," in *IPCC Special Report on the Ocean and Cryosphere in a Changing Climate*.

Bokulich, N. A., Subramanian, S., Faith, J. J., Gevers, D., Gordon, J. I., Knight, R., et al. (2013). Quality-filtering vastly improves diversity estimates from Illumina amplicon sequencing. *Nat. Methods* 10, 57–59. doi:10.1038/nmeth.2276.

Briand, J.-F., Barani, A., Garnier, C., Réhel, K., Urvois, F., LePoupon, C., et al. (2017). Spatio-temporal variations of marine biofilm communities colonizing artificial substrata including antifouling coatings in contrasted french coastal environments. *Microb. Ecol.* 74, 585–598. doi:10.1007/s00248-017-0966-2.

Bullock, H. A., Luo, H., and Whitman, W. B. (2017). Evolution of dimethylsulfoniopropionate metabolism in marine phytoplankton and bacteria. *Front. Microbiol.* 8, 637. doi:10.3389/fmicb.2017.00637.

Campbell, A. H., Harder, T., Nielsen, S., Kjelleberg, S., and Steinberg, P. D. (2011). Climate change and disease: bleaching of a chemically defended seaweed. *Glob. Change Biol.* 17, 2958–2970. doi:10.1111/j.1365-2486.2011.02456.x.

Campbell, A. H., Vergés, A., and Steinberg, P. D. (2014). Demographic consequences of disease in a habitat-forming seaweed and impacts on interactions between natural enemies. *Ecology* 95, 142–152.

Carriot, N., Paix, B., Greff, S., Viguier, B., Briand, J.-F., and Culioli, G. (2021). Integration of LC/MS-based molecular networking and classical phytochemical approach allows in-depth annotation of the metabolome of non-model organisms - The case study of the brown seaweed *Taonia atomaria*. *Talanta* 225, 121925. doi:10.1016/j.talanta.2020.121925.

Case, R. J., Longford, S. R., Campbell, A. H., Low, A., Tujula, N., Steinberg, P. D., et al. (2011). Temperature induced bacterial virulence and bleaching disease in a chemically defended marine macroalga. *Environ. Microbiol.* 13, 529–537. doi:10.1111/j.1462-2920.2010.02356.x.

Collins, M., Knutti, R., Arblaster, J., Dufresne, J.-L., Fichefet, T., Friedlingstein, P., et al. (2013). "Chapter 12: Long-term climate change: Projections, commitments and irreversibility," in *IPCC, 2013: Climate Change 2013: The Physical Science Basis. Contribution of Working Group I to the Fifth Assessment Report of the Intergovernmental Panel on Climate Change*.

Cram, J. A., Parada, A. E., and Fuhrman, J. A. (2016). Dilution reveals how viral lysis and grazing shape microbial communities. *Limnol. Oceanogr.* 61, 889–905. doi:https://doi.org/10.1002/lno.10259.

Curson, A. R. J., Rogers, R., Todd, J. D., Brearley, C. A., and Johnston, A. W. B. (2008). Molecular genetic analysis of a dimethylsulfoniopropionate lyase that liberates the climate-changing gas dimethylsulfide in several marine alpha-proteobacteria and *Rhodobacter sphaeroides*. *Environ. Microbiol.* 10, 757–767. doi:10.1111/j.1462-2920.2007.01499.x.

Curson, A. R. J., Todd, J. D., Sullivan, M. J., and Johnston, A. W. B. (2011). Catabolism of dimethylsulphoniopropionate: microorganisms, enzymes and genes. *Nat. Rev. Microbiol.* 9, 849–859. doi:10.1038/nrmicro2653.

Dittami, S. M., Eveillard, D., and Tonon, T. (2014). A metabolic approach to study algal–bacterial interactions in changing environments. *Mol. Ecol.* 23, 1656–1660. doi:10.1111/mec.12670.

Dogs, M., Wemheuer, B., Wolter, L., Bergen, N., Daniel, R., Simon, M., et al. (2017). Rhodobacteraceae on the marine brown alga *Fucus spiralis* are predominant and show physiological adaptation to an epiphytic lifestyle. *Syst. Appl. Microbiol.* 40, 370–382. doi:10.1016/j.syapm.2017.05.006.

Egan, S., Fernandes, N. D., Kumar, V., Gardiner, M., and Thomas, T. (2014). Bacterial pathogens, virulence mechanism and host defence in marine macroalgae. *Environ. Microbiol.* 16, 925–938. doi:10.1111/1462-2920.12288.

865 Egan, S., and Gardiner, M. (2016). Microbial dysbiosis: rethinking disease in marine ecosystems.
866 *Front. Microbiol.* 7, 991. doi:10.3389/fmicb.2016.00991.

867 Egan, S., Harder, T., Burke, C., Steinberg, P., Kjelleberg, S., and Thomas, T. (2013). The seaweed
868 holobiont: understanding seaweed–bacteria interactions. *FEMS Microbiol. Rev.* 37, 462–
869 476. doi:10.1111/1574-6976.12011.

870 Eggert, A. (2012). "Seaweed responses to temperature," in *Seaweed Biology: Novel Insights into*
871 *Ecophysiology, Ecology and Utilization* Ecological Studies., eds. C. Wiencke and K. Bischof
872 (Berlin, Heidelberg: Springer), 47–66. doi:10.1007/978-3-642-28451-9_3.

873 Escudié, F., Auer, L., Bernard, M., Mariadassou, M., Cauquil, L., Vidal, K., et al. (2018). FROGS: Find,
874 Rapidly, OTUs with Galaxy Solution. *Bioinformatics* 34, 1287–1294.
875 doi:10.1093/bioinformatics/btx791.

876 Favre, L., Ortalo-Magné, A., Greff, S., Pérez, T., Thomas, O. P., Martin, J.-C., et al. (2017).
877 Discrimination of four marine biofilm-forming bacteria by LC-MS metabolomics and
878 influence of culture parameters. *J. Proteome Res.* 16, 1962–1975.
879 doi:10.1021/acs.jproteome.6b01027.

880 Fernandes, N., Case, R. J., Longford, S. R., Seyedsayamdost, M. R., Steinberg, P. D., Kjelleberg, S.,
881 et al. (2011). Genomes and virulence factors of novel bacterial pathogens causing
882 bleaching disease in the marine red alga *Delisea pulchra*. *PLoS One* 6, e27387.
883 doi:10.1371/journal.pone.0027387.

884 Florez, J. Z., Camus, C., Hengst, M. B., Marchant, F., and Buschmann, A. H. (2019). Structure of the
885 epiphytic bacterial communities of *Macrocystis pyrifera* in localities with contrasting
886 nitrogen concentrations and temperature. *Algal Res.* 44, 101706.
887 doi:10.1016/j.algal.2019.101706.

888 Forster, R. M., and Dring, M. J. (1994). Influence of blue light on the photosynthetic capacity of
889 marine plants from different taxonomic, ecological and morphological groups. *European*
890 *Journal of Phycology* 29, 21–27. doi:10.1080/09670269400650441.

891 Fuchs, B. M., Spring, S., Teeling, H., Quast, C., Wulf, J., Schattenhofer, M., et al. (2007).
892 Characterization of a marine gammaproteobacterium capable of aerobic anoxygenic
893 photosynthesis. *Proc Natl Acad Sci U S A* 104, 2891–2896. doi:10.1073/pnas.0608046104.

894 Gardiner, M., Bournazos, A. M., Maturana-Martinez, C., Zhong, L., and Egan, S. (2017).
895 Exoproteome analysis of the seaweed pathogen *Nautella italica* R11 reveals temperature-
896 dependent regulation of RTX-like proteins. *Front. Microbiol.* 8.
897 doi:10.3389/fmicb.2017.01203.

898 Ghaderiardakani, F., Califano, G., Mohr, J. F., Abreu, M. H., Coates, J. C., and Wichard, T. (2019).
899 Analysis of algal growth- and morphogenesis-promoting factors in an integrated multi-

trophic aquaculture system for farming *Ulva* spp. *Aquac. Environ. Interact.* 11, 375–391. doi:10.3354/aei00319.

Ghaderiardakani, F., Coates, J. C., and Wichard, T. (2017). Bacteria-induced morphogenesis of *Ulva intestinalis* and *Ulva mutabilis* (Chlorophyta): a contribution to the lottery theory. *FEMS Microbiol. Ecol.* 93. doi:10.1093/femsec/fix094.

Gobet, A., Barbeyron, T., Matard-Mann, M., Magdelenat, G., Vallenet, D., Duchaud, E., et al. (2018). Evolutionary evidence of algal polysaccharide degradation acquisition by *Pseudoalteromonas carrageenovora* 9T to adapt to macroalgal niches. *Front. Microbiol.* 9, 2740. doi:10.3389/fmicb.2018.02740.

Groisillier, A., Labourel, A., Michel, G., and Tonon, T. (2015). The mannitol utilization system of the marine bacterium *Zobellia galactanivorans*. *Appl. Environ. Microbiol.* 81, 1799–1812. doi:10.1128/AEM.02808-14.

Grosser, K., Zedler, L., Schmitt, M., Dietzek, B., Popp, J., and Pohnert, G. (2012). Disruption-free imaging by Raman spectroscopy reveals a chemical sphere with antifouling metabolites around macroalgae. *Biofouling* 28, 687–696. doi:10.1080/08927014.2012.700306.

Guiry, M. D., and Guiry, M. D. (2020). *AlgaeBase*. World-wide electronic publication, National University of Ireland, Galway. https://www.algaebase.org; searched on 05 June 2020.

Hanelt, D., Uhrmacher, S., and Nultsch, W. (1995). The effect of photoinhibition on photosynthetic oxygen production in the brown alga *Dictyota dichotoma*. *Botanica Acta* 108, 99–105. doi:10.1111/j.1438-8677.1995.tb00838.x.

Harder, T., Campbell, A. H., Egan, S., and Steinberg, P. D. (2012). Chemical mediation of ternary interactions between marine holobionts and their environment as exemplified by the red alga *Delisea pulchra*. *J. Chem. Ecol.* 38, 442–450. doi:10.1007/s10886-012-0119-5.

Hartmann, A., Albert, A., and Ganzera, M. (2015). Effects of elevated ultraviolet radiation on primary metabolites in selected alpine algae and cyanobacteria. *J. Photochem. Photobiol. B* 149, 149–155. doi:10.1016/j.jphotobiol.2015.05.016.

Heo, S.-J., and Jeon, Y.-J. (2009). Protective effect of fucoxanthin isolated from *Sargassum siliquastrum* on UV-B induced cell damage. *J. Photochem. Photobiol. B* 95, 101–107. doi:10.1016/j.jphotobiol.2008.11.011.

Hollants, J., Leliaert, F., De Clerck, O., and Willems, A. (2013). What we can learn from sushi: a review on seaweed-bacterial associations. *FEMS Microbiol. Ecol.* 83, 1–16. doi:10.1111/j.1574-6941.2012.01446.x.

Howard, E. C., Sun, S., Biers, E. J., and Moran, M. A. (2008). Abundant and diverse bacteria involved in DMSP degradation in marine surface waters. *Environ. Microbiol.* 10, 2397–2410. doi:10.1111/j.1462-2920.2008.01665.x.

935 Huggett, M. J., McMahon, K., and Bernasconi, R. (2018). Future warming and acidification result
936 in multiple ecological impacts to a temperate coralline alga. *Environ. Microbiol.* 20, 2769–
937 2782. doi:10.1111/1462-2920.14113.

938 Inaba, M., Suzuki, I., Szalontai, B., Kanesaki, Y., Los, D. A., Hayashi, H., et al. (2003). Gene-
939 engineered rigidification of membrane lipids enhances the cold inducibility of gene
940 expression in *Synechocystis*. *J. Biol. Chem.* 278, 12191–12198.
941 doi:10.1074/jbc.M212204200.

942 Karsten, U., Kirst, G. O., and Wiencke, C. (1992). Dimethylsulphoniopropionate (DMSP)
943 accumulation in green macioalgae from polar to temperate regions: interactive effects of
944 light versus salinity and light versus temperature. *Polar Biol.* 12, 603–607.
945 doi:10.1007/BF00236983.

946 Karsten, U., Wiencke, C., and Kirst, G. O. (1990). The effect of light intensity and daylength on the
947 *β*-dimethylsulphoniopropionate (DMSP) content of marine green macroalgae from
948 Antarctica. *Plant Cell Environ.* 13, 989–993. doi:10.1111/j.1365-3040.1990.tb01991.x.

949 Kessler, R. W., Weiss, A., Kuegler, S., Hermes, C., and Wichard, T. (2018). Macroalgal-bacterial
950 interactions: Role of dimethylsulfoniopropionate in microbial gardening by *Ulva*
951 (Chlorophyta). *Mol. Ecol.* 27, 1808–1819. doi:10.1111/mec.14472.

952 Kets, E. P., Galinski, E. A., de Wit, M., de Bont, J. A., and Heipieper, H. J. (1996). Mannitol, a novel
953 bacterial compatible solute in *Pseudomonas putida* S12. *J. Bacteriol.* 178, 6665–6670.
954 doi:10.1128/jb.178.23.6665-6670.1996.

955 Koblížek, M. (2015). Ecology of aerobic anoxygenic phototrophs in aquatic environments. *FEMS*
956 *Microbiol. Rev.* 39, 854–870. doi:10.1093/femsre/fuv032.

957 Kumar, V., Zozaya-Valdes, E., Kjelleberg, S., Thomas, T., and Egan, S. (2016). Multiple opportunistic
958 pathogens can cause a bleaching disease in the red seaweed *Delisea pulchra*. *Environ.*
959 *Microbiol.* 18, 3962–3975. doi:10.1111/1462-2920.13403.

960 Lachnit, T., Fischer, M., Künzel, S., Baines, J. F., and Harder, T. (2013). Compounds associated with
961 algal surfaces mediate epiphytic colonization of the marine macroalga *Fucus vesiculosus*.
962 *FEMS Microbiol. Ecol.* 84, 411–420. doi:10.1111/1574-6941.12071.

963 Lachnit, T., Wahl, M., and Harder, T. (2010). Isolated thallus-associated compounds from the
964 macroalga *Fucus vesiculosus* mediate bacterial surface colonization in the field similar to
965 that on the natural alga. *Biofouling* 26, 247–255. doi:10.1080/08927010903474189.

966 Lawes, J. C., Neilan, B. A., Brown, M. V., Clark, G. F., and Johnston, E. L. (2016). Elevated nutrients
967 change bacterial community composition and connectivity: high throughput sequencing
968 of young marine biofilms. *Biofouling* 32, 57–69. doi:10.1080/08927014.2015.1126581.

969 Lehvo, A., Bäck, S., and Kiirikki, M. (2001). Growth of *Fucus vesiculosus* L. (Phaeophyta) in the
970 Northern Baltic proper: Energy and nitrogen storage in seasonal environment. *Botanica*
971 *Marina* 44, 345–350. doi:10.1515/BOT.2001.044.

972 Longford, S. R., Campbell, A. H., Nielsen, S., Case, R. J., Kjelleberg, S., and Steinberg, P. D. (2019).
973 Interactions within the microbiome alter microbial interactions with host chemical
974 defences and affect disease in a marine holobiont. *Sci. Rep.* 9, 1363. doi:10.1038/s41598-
975 018-37062-z.

976 Loreau, M., Naeem, S., Inchausti, P., Bengtsson, J., Grime, J. P., Hector, A., et al. (2001).
977 Biodiversity and ecosystem functioning: current knowledge and future challenges. *Science*
978 294, 804–808. doi:10.1126/science.1064088.

979 Los, D. A., and Murata, N. (2004). Membrane fluidity and its roles in the perception of
980 environmental signals. *Biochim. Biophys. Acta* 1666, 142–157.
981 doi:10.1016/j.bbamem.2004.08.002.

982 Lyons, D. A., Scheibling, R. E., and Alstyne, K. L. V. (2010). Spatial and temporal variation in DMSP
983 content in the invasive seaweed *Codium fragile* ssp. *fragile*: effects of temperature, light
984 and grazing. *Mar. Ecol. Prog. Ser.* 417, 51–61. doi:10.3354/meps08818.

985 Mahé, F., Rognes, T., Quince, C., Vargas, C. de, and Dunthorn, M. (2014). Swarm: robust and fast
986 clustering method for amplicon-based studies. *PeerJ* 2, e593. doi:10.7717/peerj.593.

987 Martin, S., Castets, M.-D., and Clavier, J. (2006). Primary production, respiration and calcification
988 of the temperate free-living coralline alga *Lithothamnion corallioides*. *Aquat. Bot.* 85, 121–
989 128. doi:10.1016/j.aquabot.2006.02.005.

990 Maximilien, R., Nys, R. de, Holmstrm, C., Gram, L., Givskov, M., Crass, K., et al. (1998). Chemical
991 mediation of bacterial surface colonisation by secondary metabolites from the red alga
992 *Delisea pulchra*. *Aquat. Microb. Ecol.* 15, 233–246. doi:10.3354/ame015233.

993 McMurdie, P. J., and Holmes, S. (2013). phyloseq: an R package for reproducible interactive
994 analysis and graphics of microbiome census data. *PLoS One* 8, e61217.
995 doi:10.1371/journal.pone.0061217.

996 Mensch, B., Neulinger, S. C., Graiff, A., Pansch, A., Künzel, S., Fischer, M. A., et al. (2016).
997 Restructuring of epibacterial communities on *Fucus vesiculosus* forma *mytili* in response
998 to elevated pCO_2 and increased temperature levels. *Front. Microbiol.* 7, 434.
999 doi:10.3389/fmicb.2016.00434.

1000 Minich, J. J., Morris, M. M., Brown, M., Doane, M., Edwards, M. S., Michael, T. P., et al. (2018).
1001 Elevated temperature drives kelp microbiome dysbiosis, while elevated carbon dioxide
1002 induces water microbiome disruption. *PLoS One* 13, e0192772.
1003 doi:10.1371/journal.pone.0192772.

1004 Moore, P. D. (2005). Roots of stability. *Nature* 437, 959–961. doi:10.1038/437959a.

1005 Mou, X., Moran, M. A., Stepanauskas, R., González, J. M., and Hodson, R. E. (2005). Flow-
1006 cytometric cell sorting and subsequent molecular analyses for culture-independent
1007 identification of bacterioplankton involved in dimethylsulfoniopropionate
1008 transformations. *Appl. Environ. Microbiol.* 71, 1405–1416. doi:10.1128/AEM.71.3.1405-
1009 1416.2005.

1010 Murakami, H., Serisawa, Y., Kurashima, A., and Yokohama, Y. (2004). Photosynthetic
1011 performances of temperate *Sargassum* and Kelp species growing in the same habitat.
1012 *Algae* 19, 207–216.

1013 Othmani, A., Briand, J.-F., Ayé, M., Molmeret, M., and Culioli, G. (2016). Surface metabolites of
1014 the brown alga *Taonia atomaria* have the ability to regulate epibiosis. *Biofouling* 32, 801–
1015 813. doi:10.1080/08927014.2016.1198954.

1016 Paix, B., Carriot, N., Barry-Martinet, R., Greff, S., Misson, B., Briand, J.-F., et al. (2020). A multi-
1017 omics analysis suggests links between the differentiated surface metabolome and
1018 epiphytic microbiota along the thallus of a Mediterranean seaweed holobiont. *Front.*
1019 *Microbiol.* 11, 494. doi:10.3389/fmicb.2020.00494.

1020 Paix, B., Layglon, N., Le Poupon, C., D'Onofrio, S., Misson, B., Garnier, C., et al. (*submitted*). A
1021 multi-omics approach deciphers how temperature and copper stress shape seaweed-
1022 microbiota interactions at the surface of *Taonia atomaria* on the NW Mediterranean
1023 coast. *Submitted to* Microbiome.

1024 Paix, B., Othmani, A., Debroas, D., Culioli, G., and Briand, J.-F. (2019). Temporal covariation of
1025 epibacterial community and surface metabolome in the Mediterranean seaweed
1026 holobiont *Taonia atomaria*. *Environ. Microbiol.* 21, 3346–3363. doi:10.1111/1462-
1027 2920.14617.

1028 Parada, A. E., Needham, D. M., and Fuhrman, J. A. (2016). Every base matters: assessing small
1029 subunit rRNA primers for marine microbiomes with mock communities, time series and
1030 global field samples. *Environ. Microbiol.* 18, 1403–1414. doi:10.1111/1462-2920.13023.

1031 Perez-Bermudez, P., Garcia-Carrascosa, M., Cornejo, M. J., and Segura, J. (1981). Water-depth
1032 effects in photosynthetic pigment content of the benthic algae *Dictyota dichotoma* and
1033 *Udotea petiolata*. *Aquat. Bot.* 11, 373–377. doi:10.1016/0304-3770(81)90070-X.

1034 Pitlik, S. D., and Koren, O. (2017). How holobionts get sick-toward a unifying scheme of disease.
1035 *Microbiome* 5, 64. doi:10.1186/s40168-017-0281-7.

1036 Pujalte, M. J., Lucena, T., Ruvira, M. A., Arahal, D. R., and Macián, M. C. (2014). "The family
1037 Rhodobacteraceae," in *The Prokaryotes: Alphaproteobacteria and Betaproteobacteria*,
1038 eds. E. Rosenberg, E. F. DeLong, S. Lory, E. Stackebrandt, and F. Thompson (Berlin,
1039 Heidelberg: Springer), 439–512. doi:10.1007/978-3-642-30197-1_377.

1040 Qiu, Z., Coleman, M. A., Provost, E., Campbell, A. H., Kelaher, B. P., Dalton, S. J., et al. (2019).
1041 Future climate change is predicted to affect the microbiome and condition of habitat-
1042 forming kelp. *Proc. Biol. Sci.* 286, 20181887. doi:10.1098/rspb.2018.1887.

1043 Ramus, J., Lemons, F., and Zimmerman, C. (1977). Adaptation of light-harvesting pigments to
1044 downwelling light and the consequent photosynthetic performance of the eulittoral
1045 rockweeds *Ascophyllum nodosum* and *Fucus vesiculosus*. *Mar. Biol.* 42, 293–303.
1046 doi:10.1007/BF00402191.

1047 Roberts, E. M., Bowers, D. G., and Davies, A. J. (2018). Tidal modulation of seabed light and its
1048 implications for benthic algae. *Limnology and Oceanography* 63, 91–106.
1049 doi:10.1002/lno.10616.

1050 Rognes, T., Flouri, T., Nichols, B., Quince, C., and Mahé, F. (2016). VSEARCH: a versatile open
1051 source tool for metagenomics. *PeerJ* 4, e2584. doi:10.7717/peerj.2584.

1052 Romera-Castillo, C., Sarmento, H., Alvarez-Salgado, X. A., Gasol, J. M., and Marrasé, C. (2011). Net
1053 production and consumption of fluorescent colored dissolved organic matter by natural
1054 bacterial assemblages growing on marine phytoplankton exudates. *Appl. Environ.*
1055 *Microbiol.* 77, 7490–7498. doi:10.1128/AEM.00200-11.

1056 Roth-Schulze, A. J., Pintado, J., Zozaya-Valdés, E., Cremades, J., Ruiz, P., Kjelleberg, S., et al. (2018).
1057 Functional biogeography and host specificity of bacterial communities associated with the
1058 Marine Green Alga *Ulva* spp. *Mol. Ecol.* 27, 1952–1965. doi:10.1111/mec.14529.

1059 Rousvoal, S., Groisillier, A., Dittami, S. M., Michel, G., Boyen, C., and Tonon, T. (2011). Mannitol-
1060 1-phosphate dehydrogenase activity in *Ectocarpus siliculosus*, a key role for mannitol
1061 synthesis in brown algae. *Planta* 233, 261–273. doi:10.1007/s00425-010-1295-6.

1062 Saha, M., Rempt, M., Grosser, K., Pohnert, G., and Weinberger, F. (2011). Surface-associated
1063 fucoxanthin mediates settlement of bacterial epiphytes on the rockweed *Fucus*
1064 *vesiculosus*. *Biofouling* 27, 423–433. doi:10.1080/08927014.2011.580841.

1065 Saha, M., Rempt, M., Stratil, S. B., Wahl, M., Pohnert, G., and Weinberger, F. (2014). Defence
1066 chemistry modulation by light and temperature shifts and the resulting effects on
1067 associated epibacteria of *Fucus vesiculosus*. *PLoS One* 9, e105333.
1068 doi:10.1371/journal.pone.0105333.

1069 Sand, M., Mingote, A. I., Santos, H., Müller, V., and Averhoff, B. (2013). Mannitol, a compatible
1070 solute synthesized by *Acinetobacter baylyi* in a two-step pathway including a salt-induced
1071 and salt-dependent mannitol-1-phosphate dehydrogenase. *Environ. Microbiol.* 15, 2187–
1072 2197. doi:10.1111/1462-2920.12090.

1073 Sato, N., and Murata, N. (1980). Temperature shift-induced responses in lipids in the blue-green
1074 alga, *Anabaena variabilis*: the central role of diacylmonogalactosylglycerol in thermo-
1075 adaptation. *Biochim. Biophys. Acta* 619, 353–366. doi:10.1016/0005-2760(80)90083-1.

1076 Sato, N., and Murata, N. (1982). Lipid biosynthesis in the blue-green alga, *Anabaena variabilis*: II.
1077 Fatty acids and lipid molecular species. *Biochim. Biophys. Acta* 710, 279–289.
1078 doi:10.1016/0005-2760(82)90110-2.

1079 Schäfer, H., Servais, P., and Muyzer, G. (2000). Successional changes in the genetic diversity of a
1080 marine bacterial assemblage during confinement. *Arch. Microbiol.* 173, 138–145.
1081 doi:10.1007/s002039900121.

1082 Schüler, L. M., Schulze, P. S. C., Pereira, H., Barreira, L., León, R., and Varela, J. (2017). Trends and
1083 strategies to enhance triacylglycerols and high-value compounds in microalgae. *Algal Res.*
1084 25, 263–273. doi:10.1016/j.algal.2017.05.025.

1085 Schultz-Johansen, M., Glaring, M. A., Bech, P. K., and Stougaard, P. (2016). Draft genome
1086 sequence of a novel marine bacterium, *Paraglaciecola* sp. strain s66, with hydrolytic
1087 activity against seaweed polysaccharides. *Genome Announc.* 4.
1088 doi:10.1128/genomeA.00304-16.

1089 Selyanin, V., Hauruseu, D., and Koblížek, M. (2016). The variability of light-harvesting complexes
1090 in aerobic anoxygenic phototrophs. *Photosynth. Res.* 128, 35–43. doi:10.1007/s11120-
1091 015-0197-7.

1092 Stratil, S. B., Neulinger, S. C., Knecht, H., Friedrichs, A. K., and Wahl, M. (2013). Temperature-
1093 driven shifts in the epibiotic bacterial community composition of the brown macroalga
1094 *Fucus vesiculosus*. *Microbiologyopen* 2, 338–349. doi:10.1002/mbo3.79.

1095 Tada, Y., Taniguchi, A., Nagao, I., Miki, T., Uematsu, M., Tsuda, A., et al. (2011). Differing growth
1096 responses of major phylogenetic groups of marine bacteria to natural phytoplankton
1097 blooms in the western North Pacific Ocean. *Appl. Environ. Microbiol.* 77, 4055–4065.
1098 doi:10.1128/AEM.02952-10.

1099 Ternon, E., Paix, B., Thomas, O. P., Briand, J.-F., and Culioli, G. (2020). Exploring the role of
1100 macroalgal surface metabolites on the settlement of the benthic dinoflagellate *Ostreopsis*
1101 cf. *ovata*. *Front. Mar. Sci.* 7. doi:10.3389/fmars.2020.00683.

1102 Thomas, F., Barbeyron, T., Tonon, T., Génicot, S., Czjzek, M., and Michel, G. (2012).
1103 Characterization of the first alginolytic operons in a marine bacterium: from their
1104 emergence in marine Flavobacteriia to their independent transfers to marine
1105 Proteobacteria and human gut Bacteroides. *Environ. Microbiol.* 14, 2379–2394.
1106 doi:10.1111/j.1462-2920.2012.02751.x.

1107 Thomas, F., Dittami, S. M., Brunet, M., Duff, N. L., Tanguy, G., Leblanc, C., et al. (2020). Evaluation
1108 of a new primer combination to minimize plastid contamination in 16S rDNA
1109 metabarcoding analyses of alga-associated bacterial communities. *Environ. Microbiol.*
1110 *Rep.* 12, 30–37. doi:10.1111/1758-2229.12806.

1111 Thomas, F., Lundqvist, L. C. E., Jam, M., Jeudy, A., Barbeyron, T., Sandström, C., et al. (2013).
1112 Comparative characterization of two marine alginate lyases from *Zobellia galactanivorans*
1113 reveals distinct modes of action and exquisite adaptation to their natural substrate. *J. Biol.*
1114 *Chem.* 288, 23021–23037. doi:10.1074/jbc.M113.467217.

1115 Van Alstyne, K. L., and Puglisi, M. P. (2007). DMSP in marine macroalgae and macroinvertebrates:
1116 Distribution, function, and ecological impacts. *Aquat. Sci.* 69, 394–402.
1117 doi:10.1007/s00027-007-0888-z.

1118 van der Loos, L. M., Eriksson, B. K., and Falcão Salles, J. (2019). The macroalgal holobiont in a
1119 changing sea. *Trends Microbiol.* 27, 635–650. doi:10.1016/j.tim.2019.03.002.

1120 Viano, Y., Bonhomme, D., Camps, M., Briand, J.-F., Ortalo-Magné, A., Blache, Y., et al. (2009).
1121 Diterpenoids from the Mediterranean brown alga *Dictyota* sp. evaluated as antifouling
1122 substances against a marine bacterial biofilm. *J. Nat. Prod.* 72, 1299–1304.
1123 doi:10.1021/np900102f.

1124 Wahl, M., Goecke, F., Labes, A., Dobretsov, S., and Weinberger, F. (2012). The second skin:
1125 ecological role of epibiotic biofilms on marine organisms. *Front. Microbiol.* 3, 292.
1126 doi:10.3389/fmicb.2012.00292.

1127 Webster, N. S., Soo, R., Cobb, R., and Negri, A. P. (2011). Elevated seawater temperature causes
1128 a microbial shift on crustose coralline algae with implications for the recruitment of coral
1129 larvae. *ISME J.* 5, 759–770. doi:10.1038/ismej.2010.152.

1130 Weinberger, F., Rohde, S., Oschmann, Y., Shahnaz, L., Dobretsov, S., and Wahl, M. (2011). Effects
1131 of limitation stress and of disruptive stress on induced antigrazing defense in the bladder
1132 wrack *Fucus vesiculosus*. *Mar. Ecol. Prog. Ser.* 427, 83–94. doi:10.3354/meps09044.

1133 Wichard, T., and Beemelmanns, C. (2018). Role of chemical mediators in aquatic interactions
1134 across the Prokaryote-Eukaryote boundary. *J. Chem. Ecol.* 44, 1008–1021.
1135 doi:10.1007/s10886-018-1004-7.

1136 Wichard, T., Charrier, B., Mineur, F., Bothwell, J. H., Clerck, O. D., and Coates, J. C. (2015). The
1137 green seaweed *Ulva*: a model system to study morphogenesis. *Front. Plant Sci.* 6, 72.
1138 doi:10.3389/fpls.2015.00072.

1139 Wietz, M., Duncan, K., Patin, N. V., and Jensen, P. R. (2013). Antagonistic interactions mediated
1140 by marine bacteria: the role of small molecules. *J Chem Ecol* 39, 879–891.
1141 doi:10.1007/s10886-013-0316-x.

1142 Yoon, J.-H., Kang, S.-J., Park, S., Oh, K.-H., and Oh, T.-K. (2010). *Jannaschia seohaensis* sp. nov.,
1143 isolated from a tidal flat sediment. *Int. J. Syst. Evol. Microbiol.* 60, 191–195.
1144 doi:10.1099/ijs.0.011270-0.

1145 Zahid, N., Schweiger, P., Galinski, E., and Deppenmeier, U. (2015). Identification of mannitol as
1146 compatible solute in *Gluconobacter oxydans*. *Appl. Microbiol. Biotechnol.* 99, 5511–5521.
1147 doi:10.1007/s00253-015-6626-x.

1148 Zemb, O., West, N., Bourrain, M., Godon, J. J., and Lebaron, P. (2010). Effect of a transient
1149 perturbation on marine bacterial communities with contrasting history. *J. Appl. Microbiol.*
1150 109, 751–762. doi:10.1111/j.1365-2672.2010.04706.x.

1151 Zozaya-Valdés, E., Egan, S., and Thomas, T. (2015). A comprehensive analysis of the microbial
1152 communities of healthy and diseased marine macroalgae and the detection of known and
1153 potential bacterial pathogens. *Front. Microbiol.* 6, 146. doi:10.3389/fmicb.2015.00146.

1154 Zozaya-Valdés, E., Roth-Schulze, A. J., and Thomas, T. (2016). Effects of temperature stress and
1155 aquarium conditions on the red macroalga *Delisea pulchra* and its associated microbial
1156 community. *Front. Microbiol.* 7, 161. doi:10.3389/fmicb.2016.00161.

1157

1158

Figure legends

Figure 1. Experimental design of the study. (A) Workflow of the full experiment over time. (B) Details of the waterflow circulating within the experimental devices.

Figure 2. Multivariate analyses of surface microbiota and surface metabolomes including all samples of *T. atomaria*, represented according to their sampling time. (A) weighted UniFrac based NMDS plots showing β-diversity differences of epibacterial communities. (B) PCA score plots showing differences of surface metabolomes.

Figure 3. Weighted UniFrac based NMDS plots showing differences of β-diversity of epibacterial communities of *T. atomaria* samples collected at a specific sampling time: (A) t_1, (B) t_2, and (C) t_3.

Figure 4. Summary of significant variations of discriminant bacterial genera at the surface of *T. atomaria* samples collected at t_3 according to cross-conditions of temperature and irradiance.
An arrow between two aquaria indicates a significant difference of relative abundance of a discriminant genus (Duncan's test and Benjamini-Hochberg *p*-value adjustment) between two conditions. ↗ and ↘ symbols after a genus name indicate whether a significant increase or decrease is respectively observed from the condition where the arrow starts to the condition where the arrow ends.

Figure 5. PCA score plots showing differences of surface metabolomes of *T. atomaria* depending on the sampling time: (A) t_1 samples, (B) t_2 samples, and (C) t_3 samples.

Figure 6. Summary of significant variations of discriminant surface metabolites of *T. atomaria* according to cross-conditions of temperature and irradiance at t_3.
An arrow between two aquaria indicates a significant difference of the normalized concentrations of a chemical biomarker (ANOVA and Tukey's tests) between two conditions. ↗ and ↘ symbols after a compound name indicate whether a significant increase and decrease is respectively observed, from the condition where the arrow starts to the condition where the arrow ends.

A

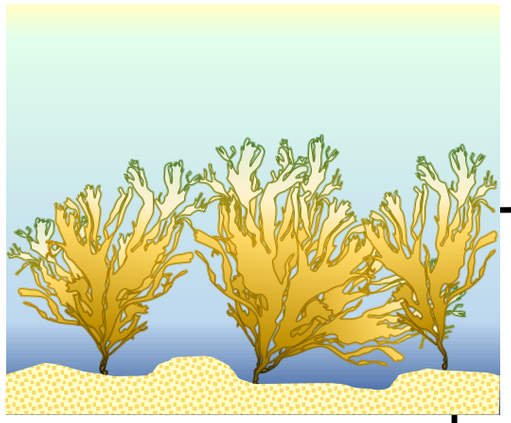

Shelve 1 Shelve 2 Shelve 3

Shelve 1 Shelve 2 Shelve 3

Sampling | Acclimatation period (7 days) | t_0 | 1 day | t_1

Field samples (n = 3)

t_0 samples (n = 3)

t_1 samples (n = 3)*9

Shelve 1 Shelve 2 Shelve 3

Shelve 1 Shelve 2 Shelve 3

7 days | t_2 | 7 days | t_3

t_2 samples (n = 3)*9

t_3 samples (n = 3)*9

Irradiance

« High » : HI

« Ambient » : AI

« Low » : LI

Temperature

« High » : HT

« Ambient » : AT

« Low » : LT

B

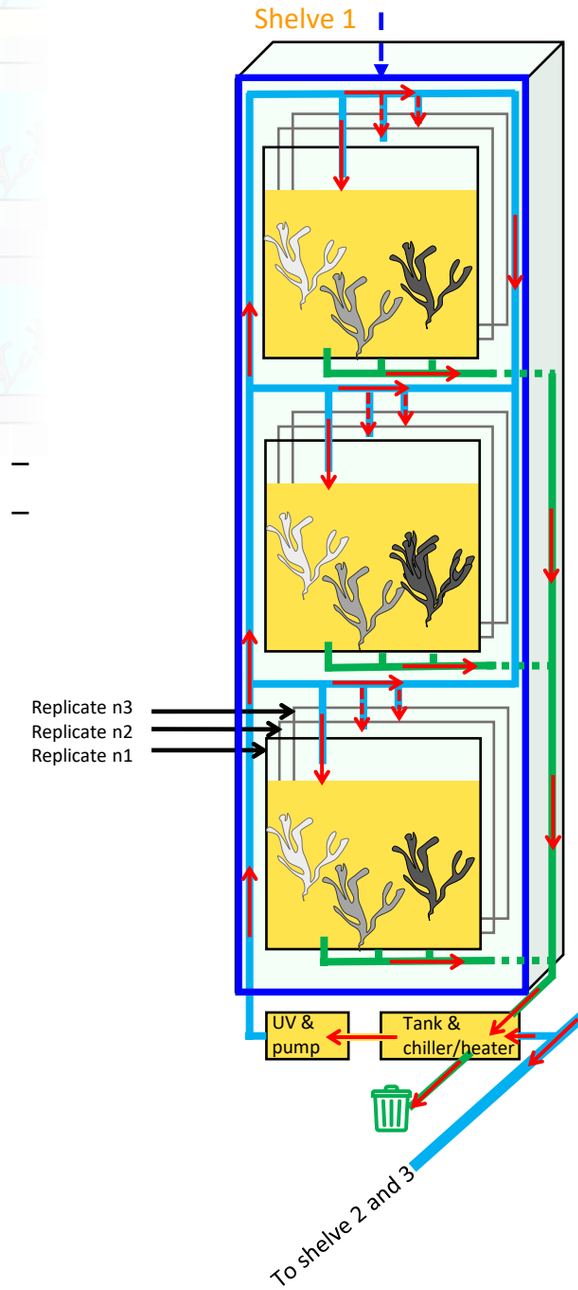

Ingoing waterflow

Outgoing waterflow

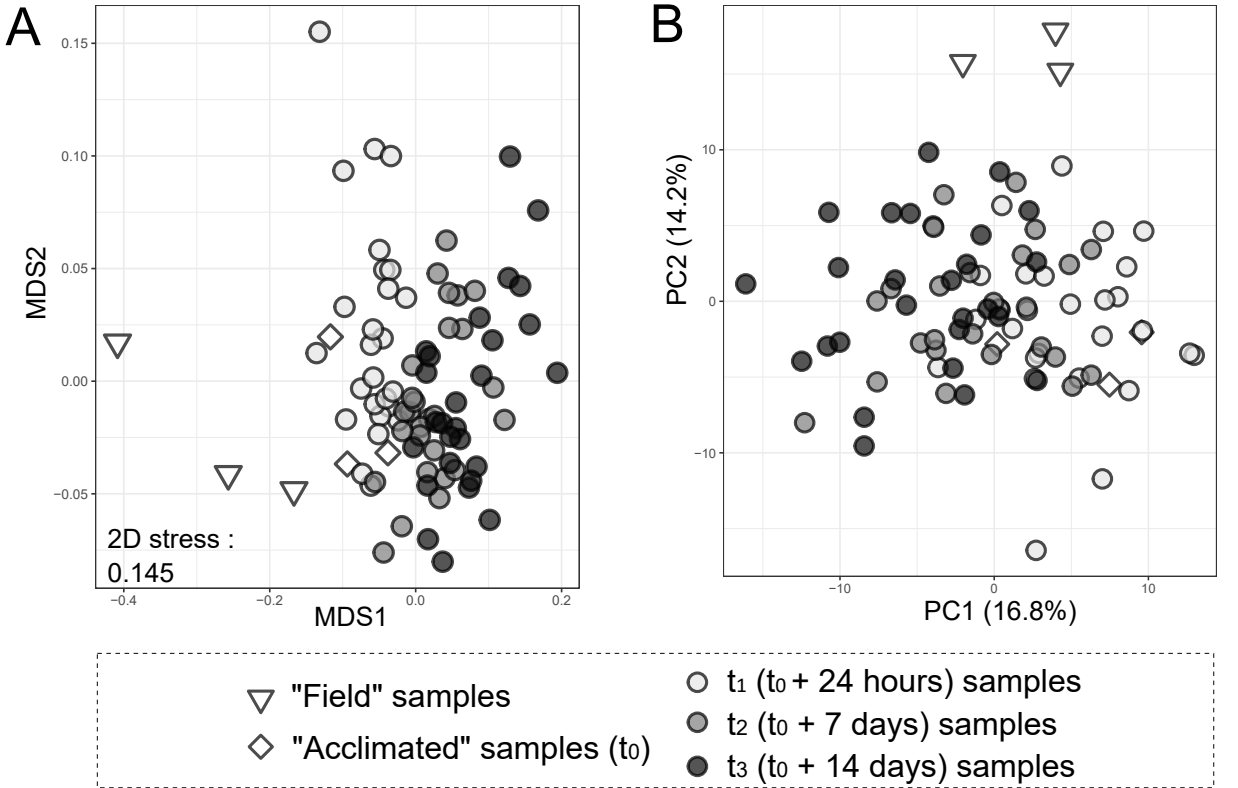
A
B
MDS2
MDS1
2D stress :
0.145
PC2 (14.2%)
PC1 (16.8%)
"Field" samples
"Acclimated" samples (t0)
t1 (t0 + 24 hours) samples
t2 (t0 + 7 days) samples
t3 (t0 + 14 days) samples

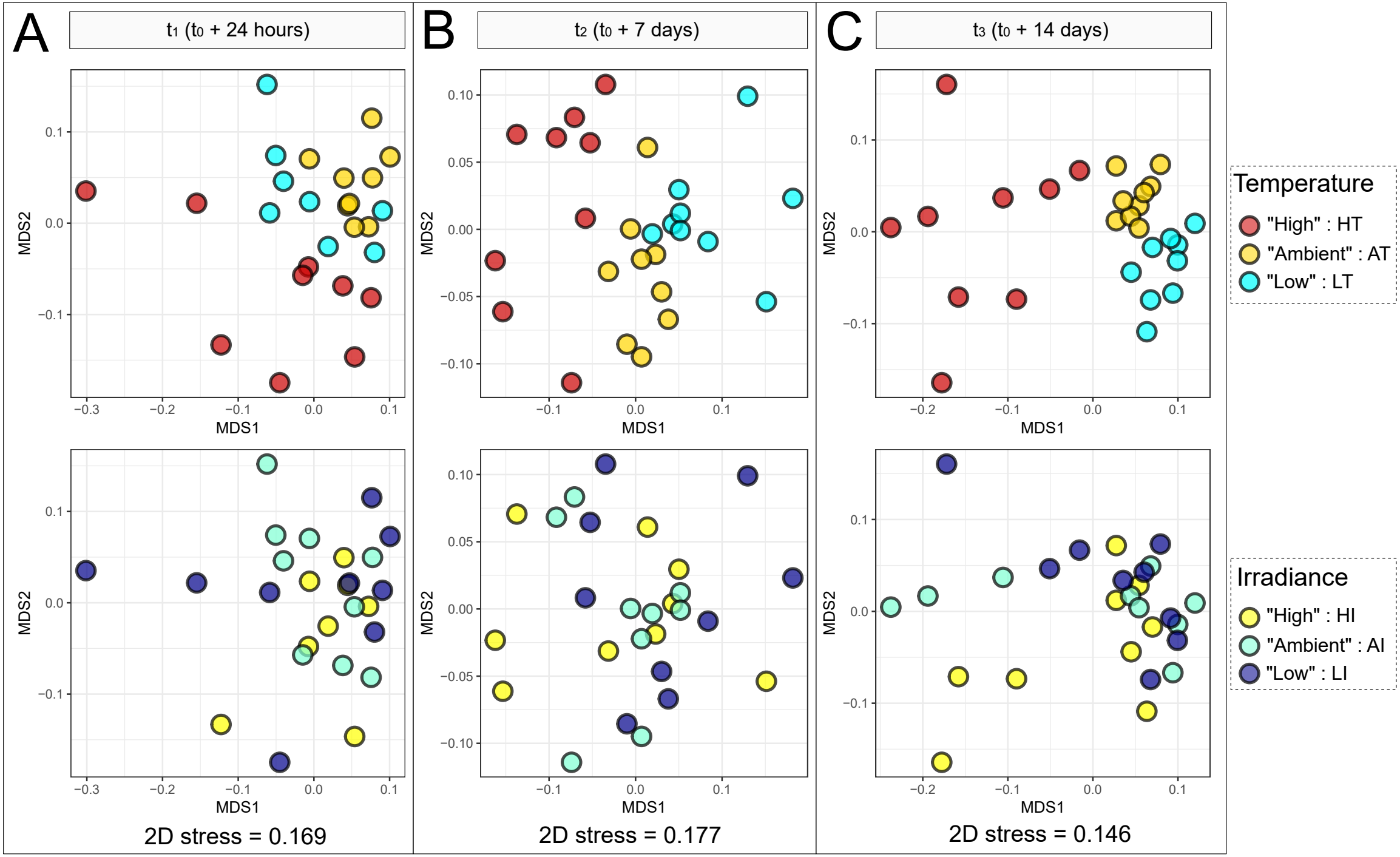
A
t1 (t0 + 24 hours)
B
t2 (t0 + 7 days)
C
t3 (t0 + 14 days)
MDS1
MDS2
2D stress = 0.169
2D stress = 0.177
2D stress = 0.146
Temperature
"High" : HT
"Ambient" : AT
"Low" : LT
Irradiance
"High" : HI
"Ambient" : AI
"Low" : LI

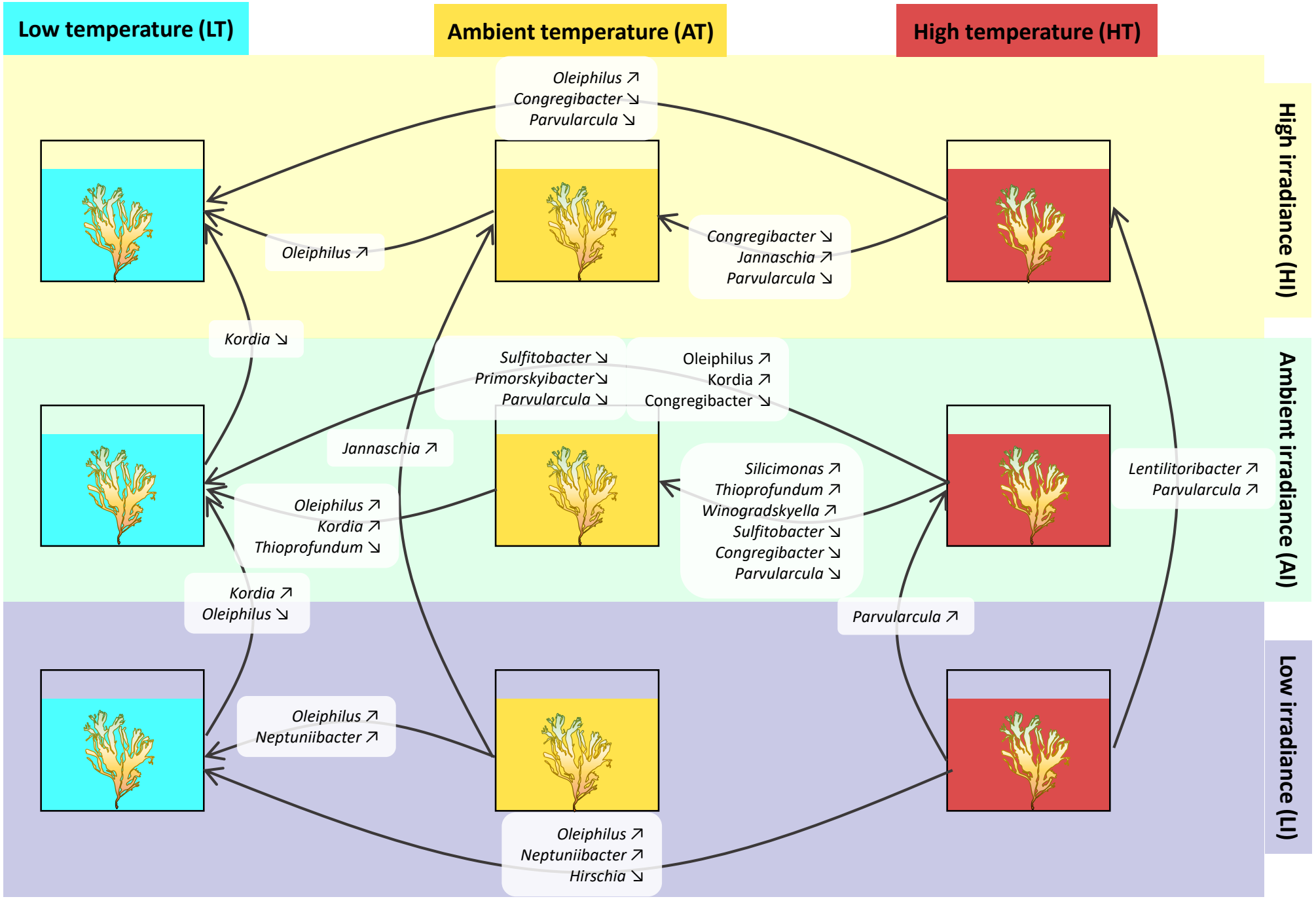
Low temperature (LT)
Ambient temperature (AT)
High temperature (HT)
High irradiance (HI)
Ambient irradiance (AI)
Low irradiance (LI)
Oleiphilus ↗
Congregibacter ↘
Parvularcula ↘
Oleiphilus ↗
Congregibacter ↘
Jannaschia ↗
Parvularcula ↘
Kordia ↘
Sulfitobacter ↘
Primorskyibacter ↘
Parvularcula ↘
Oleiphilus ↗
Kordia ↗
Congregibacter ↘
Jannaschia ↗
Oleiphilus ↗
Kordia ↗
Thioprofundum ↘
Silicimonas ↗
Thioprofundum ↗
Winogradskyella ↗
Sulfitobacter ↘
Congregibacter ↘
Parvularcula ↘
Lentilitoribacter ↗
Parvularcula ↗
Kordia ↗
Oleiphilus ↘
Parvularcula ↗
Oleiphilus ↗
Neptuniibacter ↗
Oleiphilus ↗
Neptuniibacter ↗
Hirschia ↘

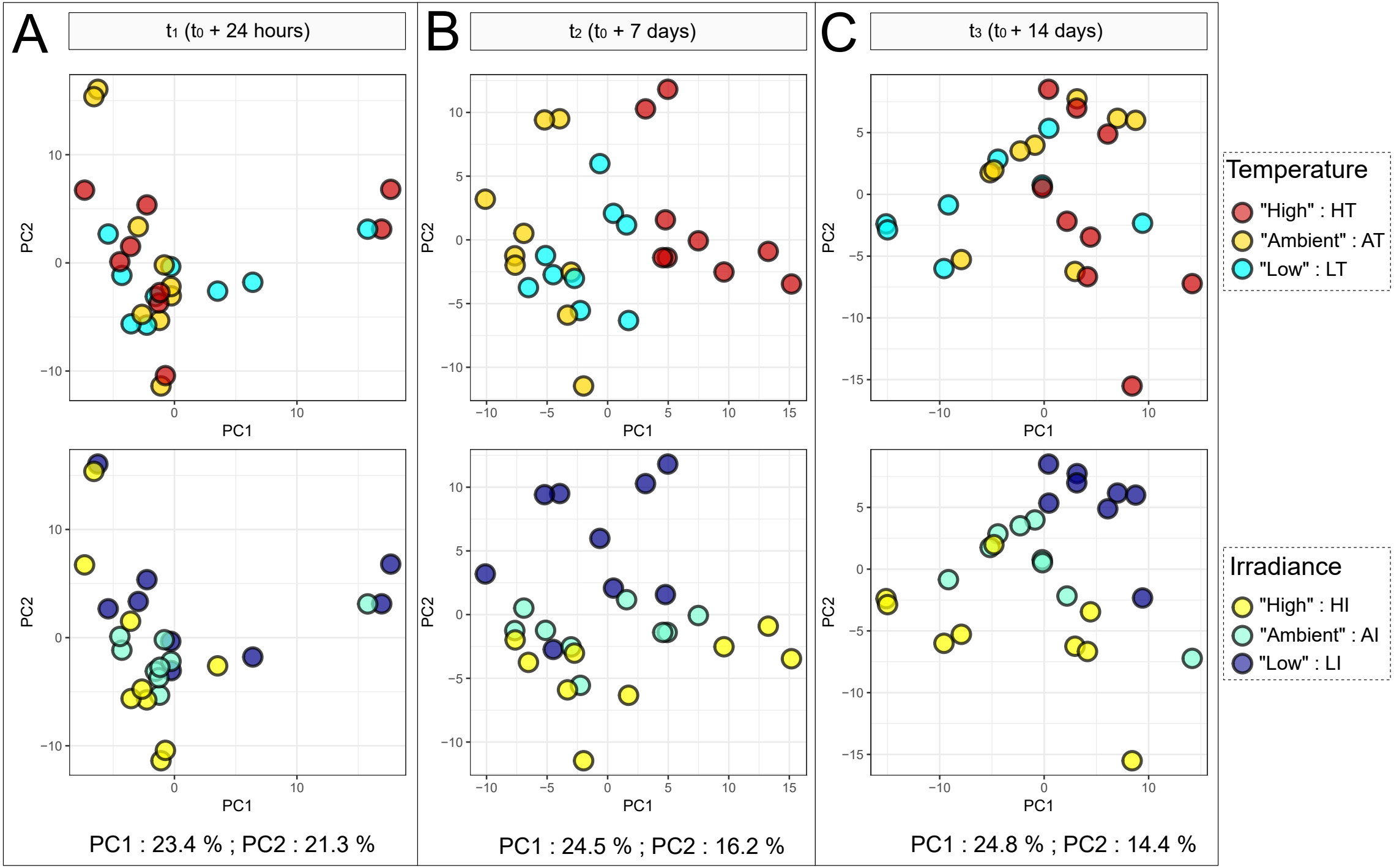
A
t1 (t0 + 24 hours)
B
t2 (t0 + 7 days)
C
t3 (t0 + 14 days)
PC1
PC2
Temperature
"High" : HT
"Ambient" : AT
"Low" : LT
Irradiance
"High" : HI
"Ambient" : AI
"Low" : LI
PC1 : 23.4 % ; PC2 : 21.3 %
PC1 : 24.5 % ; PC2 : 16.2 %
PC1 : 24.8 % ; PC2 : 14.4 %

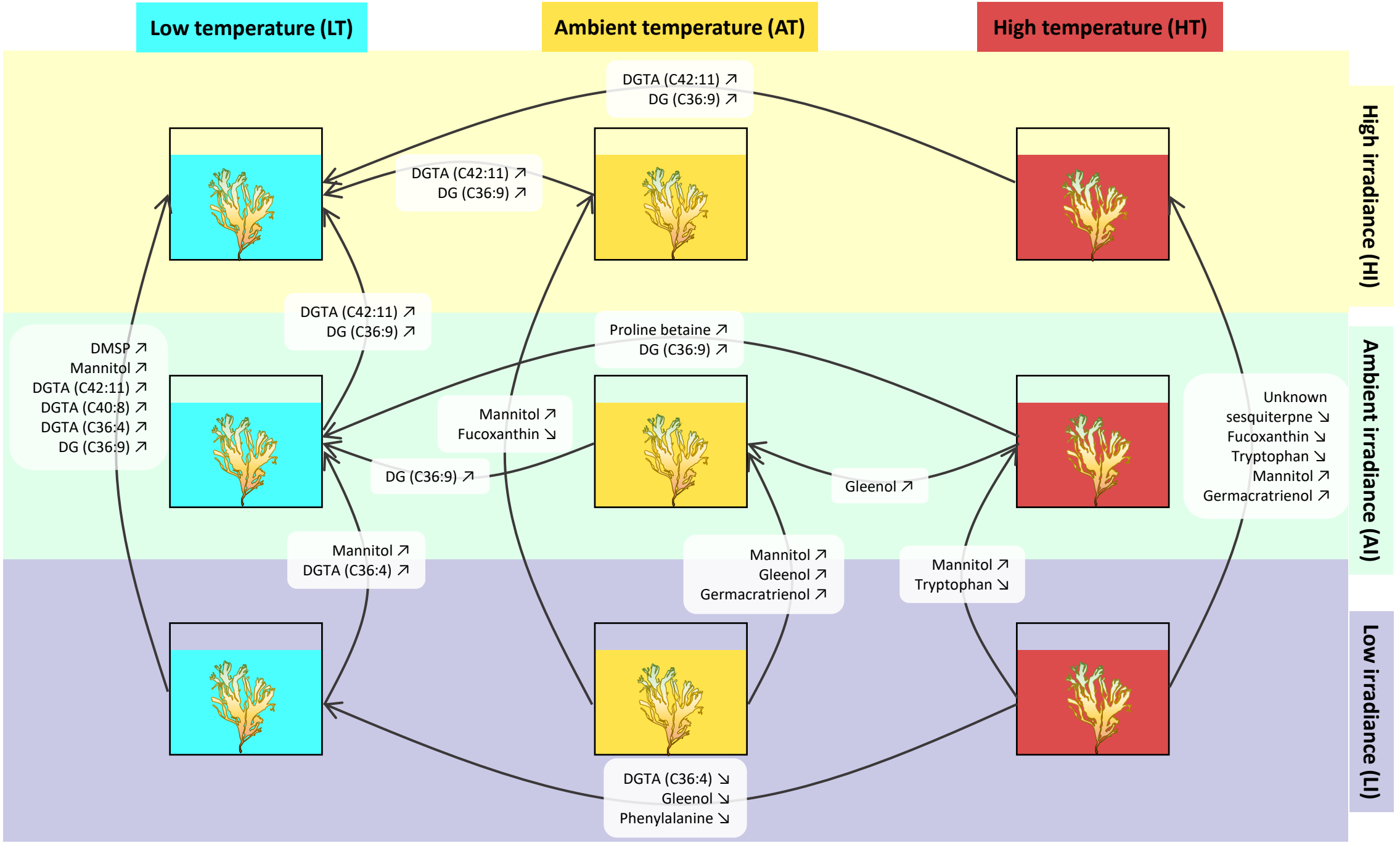
Low temperature (LT)
Ambient temperature (AT)
High temperature (HT)
High irradiance (HI)
Ambient irradiance (AI)
Low irradiance (LI)
DGTA (C42:11) ↗
DG (C36:9) ↗
DGTA (C42:11) ↗
DG (C36:9) ↗
DGTA (C42:11) ↗
DG (C36:9) ↗
Proline betaine ↗
DG (C36:9) ↗
DMSP ↗
Mannitol ↗
DGTA (C42:11) ↗
DGTA (C40:8) ↗
DGTA (C36:4) ↗
DG (C36:9) ↗
Mannitol ↗
Fucoxanthin ↘
DG (C36:9) ↗
Gleenol ↗
Unknown sesquiterpne ↘
Fucoxanthin ↘
Tryptophan ↘
Mannitol ↗
Germacratrienol ↗
Mannitol ↗
DGTA (C36:4) ↗
Mannitol ↗
Gleenol ↗
Germacratrienol ↗
Mannitol ↗
Tryptophan ↘
DGTA (C36:4) ↘
Gleenol ↘
Phenylalanine ↘